Institute of Geotechnics SAS
Košice

NŠP
National
Scholarship
Programme

МНУ
1913

POLYMER FILMS WITH INORGANIC NANOPARTICLES

Pasichnyk Mariia

2019

© 2019 Technická univerzita v Košiciach

International Standard Book Number: 978-80-553-3453-0 (Monography)

This book contains information obtained from private research.

No part of this book may be reprinted, reproduced, transmitted, or utilized in any form by any electronic, mechanical, or other means, now known or hereafter invented, including photocopying, microfilming, and recording, or in any information storage or retrieval system, without written permission from the author or publisher.

Library of Congress Cataloging-in-Publication Data
Polymer films with inorganic nanoparticles / Pasichnyk Mariia. 65 p. cm.
Includes bibliographical references and index.
ISBN **978-80-553-3453-0** (alk. paper)

Contents

Introduction

Polymer nanocomposites are commonly defined as the combination of a polymer matrix and additives that have at least one dimension in the nanometer range. The additives can be one-dimensional (examples include nanotubes and fibres), two-dimensional (which include layered minerals like clay), or three-dimensional (including spherical particles). Over the past decade, polymer nanocomposites have attracted considerable interests in both academia and industry, owing to their outstanding mechanical properties like elastic stiffness and strength with only a small amount of the nanoadditives. This is caused by the large surface area to volume ratio of nanoadditives when compared to the micro- and macro-additives. Other superior properties of polymer nanocomposites include barrier resistance, flame retardancy, scratch/wear resistance, as well as optical, magnetic and electrical properties. A typical polymer composite is a combination of a polymer and a filler. Because compounding is a technique that can ameliorate the drawbacks of conventional polymers, it has been studied over a long period and its practical applications are well known. Reinforcing materials such as `short-fiber' are often used for compounding with thermoplastic polymers in order to improve their mechanicalor thermal properties. Polyamide (nylon) is a thermoplastic polymer, and glass fiber and carbon fiber are used mainly as reinforcing materials. A filler, typically micron-sized, is incorporated into composite materials to improve their properties. The polymer matrix and the fillers are bonded to each other by weak intermolecular forces, and chemical bonding is rarely involved. If the reinforcing material in the composite could be dispersed on a molecular scale (nanometer level) and interacted with the matrix by chemical bonding, then significant improvements in the mechanical properties of the material or unexpected new properties might be realized. These are the general goals of polymer nanocomposite studies.

This book covers both fundamental and applied research associated with polymer-based nanocomposites films, and presents possible directions for further development of high performance nanocomposites.

Furthermore, the crystallization behavior of polymer/ZnO nanocomposites and the significance of chemical compatibility between a polymer and nanofiller in dispersion are also considered. Book deals with private developments of polymer nanocomposites with other nanoadditives such as ZnO and Fe_3O_4 nanoparticles. This nanoparticles, have attracted a great deal of attention because of their exceptional elastic modulus, bending strength, aspect ratio, electrical and thermal conductivity, chemical and thermal stability, and absorbability. Two chapters are entirely devoted to characterization of polymer nanocomposites. The design and fabrication of polymer nanocomposites filled with functional nanoparticles for specific functional properties, the synthesis and characterization of magnetic polymer nanocomposites, are discussed. The effect of different surface treatment techniques of Fe_3O_4 nanoparticles on the wear behavior is investigated. Styrene-acrylic polymer/Fe_3O_4 nanocomposites are described.

Acknowledgement

The author is grateful for the financial support from SAIA, n.o. within National Scholarship Program of the Slovak Republic and the VEGA 2/0156/19 project.

Nanomaterials and nanocomposition

Nanomaterials, and, in particular, nanoreinforcements for polymer composites have in recent years been the subject of intense research, development, and commercialization. Nanomaterials are an important subset of nanotechnology. Researchers are interested not only in the small dimensions that might be created, but also in the special attributes of materials whose size might be controlled to only a few atomic layers in thickness. These attributes, taken together, help to more precisely define the concept of nanomaterials. That is, nanomaterials of interest should not only have very small physical dimensions, but should also exhibit some unusual properties by virtue of their small size; and moreover, the producers of these materials should have control over the dimensions of the materials and hence the resultant property enhancements.

On this basis, it might be argued that a tire made of rubber compounded with carbon black was one of the earliest primitive nanocomposites. As early as the 1860s, the ability of carbon black to enhance the mechanical properties of vulcanized rubber was recognized by researchers who experimented with adding different materials to the basic rubber formulation. By virtue of its high surface area, surface energy, and mechanical properties, carbon black is able to significantly enhance the properties of rubber. Other well-known nanoscale reinforcements available in the early twentieth century included fumed silica and precipitated calcium carbonate. Today, industrial applications of nanomaterials can be found in a wide variety of industries. Most readers would be familiar with applications in the field of electronics and in health care. These, however, are not all. Synthetic textiles incorporating nanopowders that endow the fabrics with antibacterial, flame retardant, non-wetting, or self-cleaning properties are becoming common. Thick coatings composed of nanoparticulate metal oxides find use in waterfast ink-jet media with photo-parity, while thin coatings can be used for optical amplifying systems for light-emitting diodes. Thermal spray of nanopowders allows for the coating of flight- and land-based turbines where corrosion or erosion must be prevented. Other applications may be found in buildings and construction, in automotive and aerospace components, and in environmental remediation and energy storage technologies.

As the name suggests, polymer nanocomposites are polymer-matrix composites but contain materials having at least one dimension below about 100 nm, wherein the small size offers some level of controllable performance that is different from the expectations developed in the macroworld. The notion is that there must be some advantage in achieving the nanoscale whether it is for mechanical reinforcement or for the enhancement of another desirable property. If the nanocomposite (e.g., a polypropylene carbon nanotube composite) were to have identical properties to its macroscopic counterpart (e.g., the same polypropylene reinforced with chopped carbon fiber derived from a polyacrylonitrile precursor), then there would be little point in developing nanocomposites in the first place. The challenge, then, is to create structures either by whittling down large features or by engineering atoms such that materials and devices have novel mechanical, chemical, electrical, magnetic, or optical properties. The first nanoclay composite, in which silicates were used as a means of influencing the macroscopic properties of the composite, was described in a patent from the National Lead Company in 1950, which describes the use of clays to reinforce elastomers.

Yet, very little commercial activity proceeded from this patent, and it would be nearly four decades later before Toyota (Okada et al.) would patent a nanoclay-polyamide system in 1988, which was probably the first time that the molecular layering of silicates was recognized to be a key in transferring nano-properties to the macrocomposite. Thus, this was a true polymer nanocomposite and can be regarded as a key milestone in the modern nanocomposite era. Following this development, Toyota launched the first commercial automotive application of polymer nanoclay composites, with a Nylon-6 timing belt cover in 1993. By 2001, Toyota was producing body panels and bumpers containing nanoclays. Similarly, General Motors began using nanoclay composites for step assists on its GM Safari and Chevrolet Astro models in 2002. Special mention should be made of carbon-based nanomaterials. Prior to 1980, it was thought that only two allotropes of carbon existed: the diamond lattice and the graphite lattice. A single plane of densely packed sp^2-bonded carbon atoms arranged in a hexagonal close-packed configuration is referred to as graphene. Graphite, then, consists of multiple layers of graphene. However, by 1996 when the Nobel Prize in Chemistry was awarded to Robert F. Curl Jr., Sir Harold W. Kroto, and Richard E. Smalley, it was clear that at least a third allotrope existed—the so-called “buckyball” or C-60 atom. The nickname derives from the similarity between C-60 of the geodesic dome structures designed by the architect Buckminster Fuller. This can be considered a watershed event in the history of nanomaterials, as it catalyzed a flurry of research on nanotechnology in various fields, not only materials science. Later, other carbon molecules were discovered, such as C-72, C-76, C-84, and even as high as C-100.7 Later, as a thought experiment at least, it was suggested that single-walled carbon nanotubes (SWNTs or SWCNTs) might be considered as very large elongated fullerenes.

A SWCNT consists of a single graphene layer wrapped into a tubular shape. In practice, however, these nanomaterials are grown with the aid of a metal catalyst particle, and thus the identification of nanofilaments with fullerene molecules is mainly a theoretical one.

Electrically and thermally conductive polymer composites can be of interest for many niche applications. For example, even their weak electrical conductivity can render polymers suitable for electrostatic paint spraying, resulting in a less-expensive and an environmentally attractive process due to less wasted paint and elimination of the need for a primer coat. Alternatives such as chopped microfiber composites are not always viable due to the effect of the fibers on surface finish. Surface finish is often very important for automotive applications, obviously. Hyperion Catalysis, Inc., was one of the first producers of multiwalled nanotubes (MWNT) to bring nanocomposites to commercial status, based on the electrostatic paint spray application, as Ford Motor Company introduced MWNT nanocomposites in mirror housings on the 1998 Ford Taurus. Thus, like their nanoclay cousins, carbon nanotube composites found early commercial success in the automotive industry, at a time when many scholarly researchers were unaware that these materials had been reduced to commercial practice. This may be partly due to the innocuous trade name (Fibrils⇔) used by Hyperion to market its material.

Polymer nanocomposites

In recent years, polymer nanocomposites have attracted the attention of scientists and technologists. Significant interest in multifunctional materials caused by the desire to obtain products that would combine low cost. and a set of properties that exceeded the properties of initial components.

The rapid development of basic research has caused the creation of new multifunctional materials based on inorganic compounds with reduced dimension, can provide a wide range of properties of products from different industries.

Inorganic nanoparticles can provide specific or even unique properties to the materials, and their use in polymer composition will create coating with multifunctional properties. Thus, the introduction to the polymer composition nanoparticles of titanium oxide, zinc, or iron (III) are able to confer resistance to various types of radiation to the coating. Silver nanoparticles, are used, mainly due to their antibacterial properties. Another trend is the use of nanoparticles technology for materials, fibers containing nanoparticles coated in variety of ways. Substances that are used to modify fabrics by nanoparticles are silver and its salts, zinc oxide, copper and its oxides and others.

Modern chemical synthesis technologies provide unlimited opportunities for management of molecules structure, given the necessary properties to the created materials. Using different technologies of nanoparticles synthesis their properties can vary. However, to date there is no integrated practice of a full investigation of the structure polymer films with inorganic nanoparticles.

These films are very complex objects for research, with chaotic distribution of nanoparticles, which make it difficult to use them due to violation of the properties reproducibility and possible aggregation of nanoparticles.

The scientific approach of choosing composition components, based on their physical and chemical properties will boost volume of output and improve the quality and competitiveness of such compositions in the domestic and international markets for producing unique multifunctional materials.

In terms of nanocomposites development and management of their structure polymers represented a huge interest.

Polymer technology moving towards the creation of composite materials, in which by the directed combination of components the required set of properties are achieved. Polymer compositions obtained by finding optimal combinations of polymers and different nature fillers. Polymer films with inorganic nanoparticles should be regarded as polymer nanocomposites filled with inorganic particles with nanometer range sizes. Mechanical properties are important for such films the implementation of which can give:

- The size of nanoparticles;
- The form of nanoparticles;
- Orientation particles and their relative positions in the matrix (ordered or random, agglomeration);
- The degree of filling;
- Characteristics of the polymer matrix (binder);
- The interaction between nanoparticles and binding (strength adhesive connection, effect on the properties of nanoparticles formed by the boundary layers of polymer crystallization);
- The nature of the interaction between the polymer films and the substrate (adhesive interaction, mechanical properties, etc.).

The role of inorganic nanoparticles as fillers in the development of polymer composition is much more important as the properties of material usually depend on the relevant characteristics of nanoparticles. The molecular interaction between inorganic nanoparticles and polymer matrix, which could lead to synergies beneficial properties of organic and inorganic components in a polymer film are of great value. To describe these interactions in research we need to be involved into quantum concepts and models.

The use of filled polymeric compositions provides a production of fundamentally new multifunctional materials, improves their quality and appearance. The technology of such materials is simple and highly productive.

Polymer films containing inorganic nanoparticles tend to show stiffness increasing, yield strength and heat resistance. However, in hard polymer films nanoparticles can significantly reduce deformation and impact strength due to stress concentration that occurs on the surface of the polymer or near it. The situation can be improved by the reducing of filler particle size. In composites with elastomer binder using of inorganic nanoparticles leads to improved mechanical properties.

For example, polyurethane six-fold magnification of fracture strain and three-fold magnification of elastic constant achieved by its filling with dioxin silicon (particle size 12 nm)., in the rubber tires manufacture enhancement of caoutchouc achieved by introduction of spherical nanoparticles size up to 50 nm. For the application compositions in photonics and optoelectronics not only the nanoparticles size is important, but also an arrangement of the particles too.

The regularity between the nanoparticles size and their influence on the properties of the polymer film to this time not thoroughly investigated. After stress accommodation and initiation of deformation filler particles orientation and their connectedness changing in the material. Deformation behavior of filled highly-plastic polymers with imperfect adhesion caused by the process of phase separation and micropores formation in the material. Theoretical and experimental research shows that inorganic particles with a high geometric factors have a major enhancement effect when they are injected into the polymer matrix.

The aim of the research is the analysis of structure characteristics and components interaction in nanocomposites based on polymer matrices and inorganic nanoparticles and possibility to study the specified structure polymer films and coatings making.

To achieve this aim the objects of research were acrylic aqueous dispersion, crosslinking agent and inorganic nanoparticles.

The one that restricts the use of nanoparticles is the agglomeration, that essential decrease the properties of nanoparticles. However, agglomeration can be minimized by converting nanomaterials to nanocomposites.

In recent years, polymer nanocomposites (PNCs) have attracted the attention of scientists and technologists due to improved processability, surface area, stability, tunable properties, and cost effectiveness.

Polymer nanocomposites formed by blending inorganic nanoclusters, with organic polymers. By drying this solution polymer nanocomposite films can be formed. Such films combine two tips of properties:

- electrical, optical, magnetic and catalytic properties arising from the inorganic nanoparticles,
- enhanced thermal and mechanical stability originating from the polymeric matrix

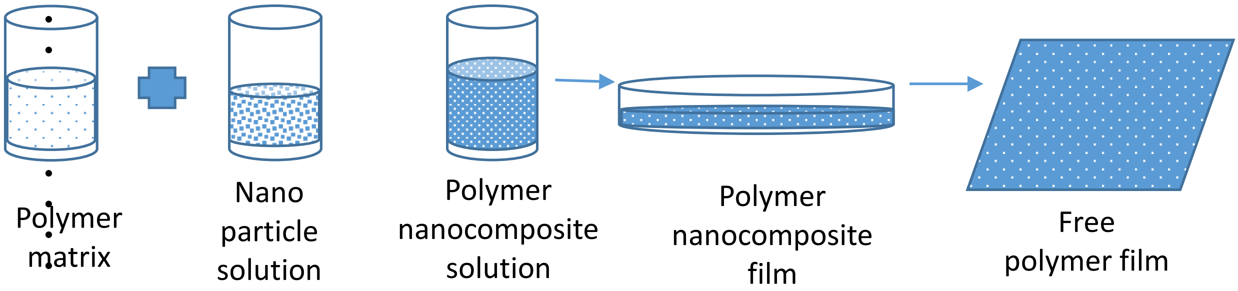

Fig. 1 Polymer nanocomposite film preparing

Polymer-metal or metal oxide nanocomposite is a new class of material that combines the advantages of both organic polymer material and inorganic metal or oxide and shows improved mechanical properties. So now basic attention is given to methods of controlled nanocomposites development with controlled given, and even better managed structure. In these cases, the process of creating nanocomposites usually consists of several stages and for purposeful creation of composites and their implementation in modern technology, it is necessary to control their structure on each stage of formation.

The properties of metal nanoparticles are highly dependent on their size and shape. Therefore, controlling the size and the shape of the metal nanoparticles has been a very significant research focus because such methods allow the fine tuning of their properties.

However, it is still difficult to design and prepare metal nanoparticles with the desired size and shape because their detailed chemistries and growth mechanisms are very complicated.

Commonly used metal oxides in polymer nanocomposites are Zinc oxide nanoparticles due to their low cost and favorable optoelectronic and catalytic properties. Nano-sized zinc oxide is more efficient at absorbing than the conventional size. In addition, it has good bactericide properties [3] and wide number of active sites. ZnO is an efficient visible-light photocatalyst and generates large quantities of hydroxyl radicals. Surface and core defects, such as oxygen vacancies, zinc interstitials, and oxygen interstitials, in ZnO play a vital role in the photocatalytic reactions by providing active sites for preventing electron–hole recombination [4]. Addition ZnO nanoparticles in the structure of polymer film let to create new class of material with improved mechanical properties, due to the forming three-dimensional structure with ZnO nanoparticles, and polymer network can prevent releasion of Zn ions and let nanoparticle to be stable.

Fe_3O_4 nanoparticles or mahnetyn characterized by low susceptibility to oxidation, high magnetic properties and low cost, besides Fe_3O_4 nanoparticles also have weak antibacterial properties.

These films are very complex objects for research, with chaotic distribution of nanoparticles, which make it difficult to use them due to violation of the properties reproducibility and possible aggregation of nanoparticles.

However, to date there is no integrated practice of a full investigation of the structure polymer films with inorganic nanoparticles.

Theoretical and experimental research shows that inorganic particles with a high geometric factors have a major enhancement effect when they are injected into the polymer matrix. In composites with elastomer binder using of inorganic nanoparticles leads to improved mechanical properties, due to the increasing cross-linking (Fig. 1).

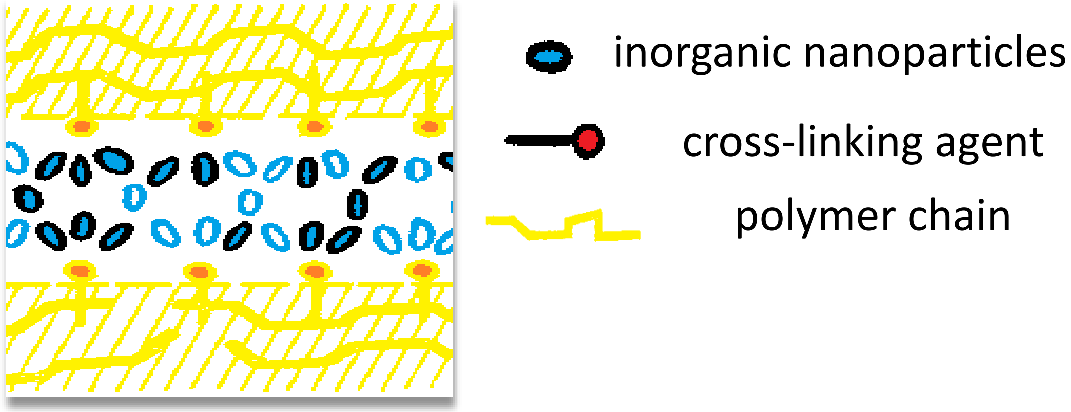

Fig. 2 Crosslinking in polymer film

Since intermolecular cross-bonds are formed by cross-linking, the linear or branched structures develop into three-dimensional polymer network that is unable to dissolve and melt.

To share the application of polymer nanocomposites its need more information about materials selection or component design. Thus, relatively little is known about such basic parameters as the degree and distribution of cross-linking as a function of network, morphology and processing conditions. This justifies the need to determine the influence of chemical bonding on cross-linking density, network structure and distribution of chains between cross-links.

However, to date there is no integrated practice of a full investigation of the structure polymer films with inorganic nanoparticles.

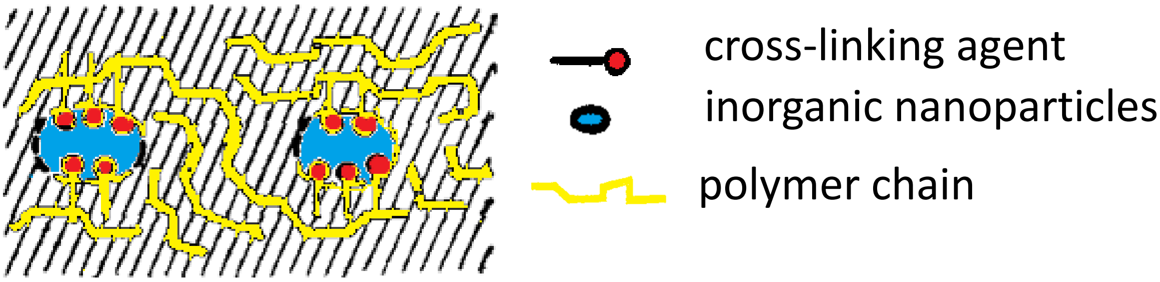

Fig. 3 Crosslinking in polymer film

The properties of polymer nanocomposites are highly dependent on the nature of the polymer (polar or non-polar), the nanofiller, the types of interaction between the filler and polymer, the nature of surface modification, and, certainly, on the distribution of the nanofiller in the polymer matrix. Depending on the distribution of the nanofiller, polymer inorganic nanocomposites are classified into three categories: intercalated nanocomposites, exfoliated nanocomposites, and immiscible nanocomposites. It has been reported that the improvement in physicochemical properties of exfoliated nanocomposites is much better in comparison to intercalated nanocomposites or conventional composites. The characterization and determination of the nanostructure of polymer/inorganic composites can be achieved using X-ray diffraction (XRD) and Fourier transform infrared spectroscopy (FT-IR).

X-ray diffraction (XRD) and transmission electron microscopy (TEM) analysis

The structure of a nanocomposite can be established by XRD. Due to the ease of use and its availability, XRD has been used widely to probe the structure of nanocomposites. When the layers are exfoliated and far apart, XRD will not show a peak in the overall diffraction diagram. In contrast, a small and broad peak is obtained at a lower angle compared with the pure nanofiller for intercalated or partially exfoliated nanocomposites. However, XRD results cannot always be taken as absolute evidence for nanolayer exfoliation, e.g. if nanofiller layers are partially exfoliated in the polymer matrix and do not have sufficiently well-defined layered structures for XRD, then the characteristic diffractions for the basal spacing cannot be detected by bulk XRD apparatus. Moreover, if the basal spacing between layers is enlarged due to the intercalation of polymer molecules, the characteristic peak will shift to a lower angle, beyond the XRD scan range (<2°).

Fourier transform infra red spectroscopy (FT-IR) analysis

The presence of a nanofiller in a polymer matrix and their interaction can be evidenced by FT-IR data analysis.

Research the crosslinking density and swelling kinetics of self-crosslinkable acrylic polymers

A variety of crosslinking reactions that can be used for acrylic dispersions have been extensively described in past years. Crosslinking method is also interesting because it can be used for in vivo conditions. The crosslinking reactions can be triggered by the evaporation of water upon drying, a change of pH or by curing at elevated temperature, where the crosslinking reaction is faster, ore reactive groups are de-blocked.

Studies on crosslinking have reported that acrylates have a good crosslinking capacity at low temperature in the field of emulsions. Furthermore most of acrylates are self-crosslinking systems where all reactive components are present and long term storage stable. Examples of suitable crosslinking systems are the reaction of the self-condensation of alkoxysilane functionality, the self-condensation of n-methylolacrylamide. Monomers such as methoxy methyl acrylate have been copolymerized with monomers containing hydroxyl groups, such as 2-hydroxyethyl acrylate (HEA), to obtain self-crosslinkable latexes.

Acrylic dispersions have found widespread uses in modern technology, due to there are key properties [1]:

- the ability to rapidly polymerization with the formation of spatially cross-linked structures,
- environmental safety dispersions of these polymers
- Resistance against household chemicals and grease
- Outdoor durability and UV resistance
- Flexibility and toughness

The physical properties of the acrylics (such as gloss, hardness, adhesion and flexibility) can be modified by altering the composition of the monomer mixture used in the polymerization process. They are frequently copolymerized with styrene, acrylonitrile, vinyl chloride or vinyl acetate, depending on the desirable properties. Some of these properties are hardness from styrene, solvent resistance from acrylonitrile, flame retardancy from vinyl chloride, and cost benefits from vinyl acetate [2].

Self-crosslinked polymer networks comprise some of the oldest and most useful polymers in modern technology. Such materials find many applications as their networks can often be made easily, with relatively little technical expertise. Unfortunately limited studies of structure-property relationships in crosslinked network have been reported for the past years.

In the same time to share the application of self-crosslinked acrylates its need more information to use as a basis for materials selection or component design. Thus, relatively little is known about such basic parameters as the degree and distribution of crosslinking as a function of network, morphology and processing conditions. This justifies the need to determine the influence of chemical bonding on crosslinking density, network structure and distribution of chains between crosslinks [3].

The following comparison of latex binder chemical types provides an indication of the relative performance, as well as the advantages and disadvantages of each type of binder. As indicated, the binder properties can be modified considerably by the presence of co-monomers. In the preset work we used aqueous dispersions Lakritex®. They are an acrylic polymers containing copolymers of styrene, butyl acrylate and acrylic acid. Lakritex 430 aqueous dispersion of copolymers of acrylic ester and styrene. Lakritex 272 aqueous dispersion of styrene-acrylic copolymer Lakritex 273, Lakritex 333 aqueous dispersion of copolymer of butyl acrylate and styrene

Crosslinking has been a significant scientific subject specific to macromolecules. From the theoretical aspects, many reports on gel network formation process have been presented since the pioneering work of Flory and Stockmayer. The classical theory has been developed by Charlesby, Scott and others. The theories make it possible to predict the relationship among molecular parameters characterizing gel such as crosslinking density, gel point, sol fraction, and degree of polymerization and molecular weight distribution of sol molecules. In addition to the network formation theory, theories on swelling and elasticity have been progressed.

In the present work, the self-crosslinking system made from aqueous dispersions Lakritex has been analyzed and compared with the theories of gel network formation and swelling. Crosslinked films (50µthick) were prepared from the aqueous dispersions Lakritex, casted on Petri dish at 80°C. The film thus obtained was heat-treated or cured for crosslinking at 150°C for 20 min inside an electric oven equipped. The four items of analysis were determined for sol and gel in the manner described in previous articles [4].

Sol-gel analysis of the polymer films was carried out by standard methods using Soxhlet apparatus. The polymer films were extracted in acetone for 18 hours and in benzene for 16 hours; after that, the mass of swollen sample and the dry residue were determined. At the stage of extraction in acetone the sol oozes – a highly-dispersed colloidal liquid solution formed from the polymer film. Using benzene at the second stage leads to initiation of coagulation contacts between particles and the formation of a gel [4]. The quantity of benzene extract (in %) corresponds to sol fraction content S:

$$S = \frac{m_a - m_b}{m_a} 100\% \qquad (1)$$

where: m_a - mass of sample after extraction in acetone, g; and m_b - mass of sample after extraction in benzene, g.

The content of sol fraction in the polymer films allows us to calculate the cross-linking degree of polymers.

The main polymer network parameters characterizing the cross-linking degree of polymer are: average molecular weight of the chain, the molecular weight of polymer cross-linked into the net, the number of net chains and the number of cross-linked molecules, the number of active chains, the fraction of active chains, the cross-linking degree.

The theory of Flory – Raineri, based on the equilibrium swelling and connecting the number of the net active chains with the relative polymer fraction in the swollen system, was used to calculate the structural parameters of the net (cross-linked polymers).

The swelling process is characterized by the swelling degree that was determined by formula:

$$a = \frac{m_2 - m_1}{m_1} 100 \qquad (2)$$

m_1 – mass of sample after swelling in benzene, g;

m_2 – mass of sample before extraction, g.

Fraction of moist-free polymer in the swollen gel was determined by the formula:

$$V_r = \frac{1}{a} \qquad (3)$$

Polymer cross-linking degree was determined by an experimentally derived number of sol fraction (S) for each film:

$$j = \frac{1}{s + \sqrt{s}} \qquad (4)$$

Fraction of active chains that are capable for cross-linking reaction was calculated by formula:

$$Vc = (1 - S)^2 (1 - 2jS)(1 + jS) \qquad (5)$$

Table 1

Network characterization of polymer films

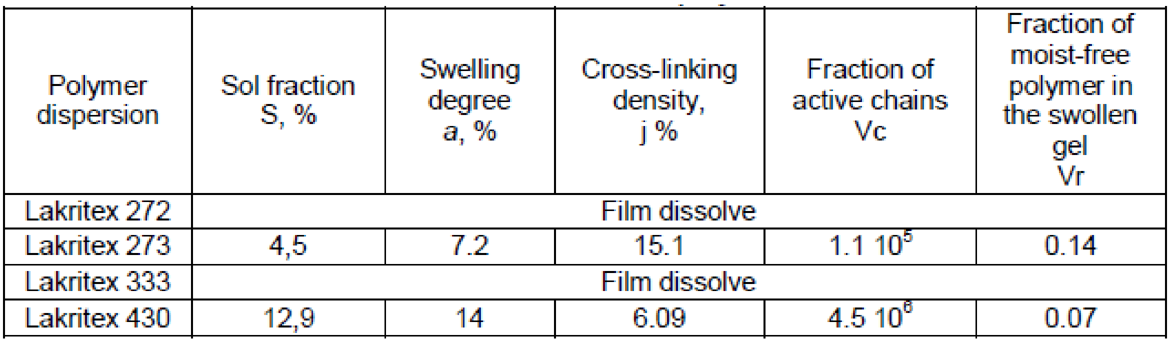

Polymer dispersion	Sol fraction S, %	Swelling degree a, %	Cross-linking density, j %	Fraction of active chains Vc	Fraction of moist-free polymer in the swollen gel Vr
Lakritex 272	Film dissolve				
Lakritex 273	4,5	7.2	15.1	$1.1\ 10^5$	0.14
Lakritex 333	Film dissolve				
Lakritex 430	12,9	14	6.09	$4.5\ 10^6$	0.07

Table 1 shows, that Lacritex 273 have higher concentration of double bonds; so the latter at equal degrees of conversion will exhibit higher density of crosslinking and will form tighter networks. Two pendant hydroxyl groups are responsible for the high water sorption and mainly for the extremely high viscosity of Lacritex 430. Lacritex 272 and Lacritex 333 with a stiff central phenyl ring core dissolve in solvents which mean that this polymers didn’t form crosslinking structure, so they are not self-crosslinkable polymers. Table summarizes the theoretical expressions for calculating various molecular parameters for crosslinked polymers based on the gel network formation theory presented by Flory, Stockmayer, Charlesby, Scott and others. The differences in the crosslinking behavior of the four acrylates studied must be due to the different chemical structure of the spacer group of acrylates and the possibility to form crosslinked network.

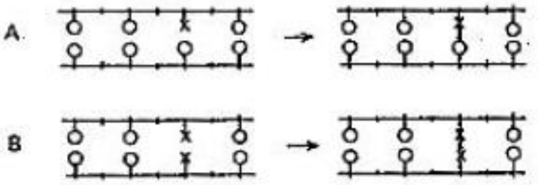

Fig. 4 Crosslinked types

A – all crosslinkable units can make crosslinking with any units in polymer;

B - crosslinkable units can make only each other

Figure 4 shows the two types of crosslinking and their effects to sol fraction, illustrated by the theoretical relationship among crosslinking density and sol fraction. The dashed lines indicate the relations in the case (A) where all crosslinkable units can make crosslinking with any units in polymer. The solid lines in the case (B) where crosslinkable units can make crosslinking only each other.

The following conclusions are obtained from the comparison of (A) and (B): Gel point, p0, the minimum value of crosslinking density p giving gel, can theoretically obtained as:

$p0 = 1/P\ w$ for (A) and $p0 = 1/\sqrt{}\ P\ w$ for (B).

Pw - weight -average degree of polymerization

For example, in the case of Lacritex 273 Pw = 2000, p0 = 0.0005 (0.025 mol% of crosslinkable units) in the case (A) while p0 = 0.024 (2.4 mol% of crosslinkable units) in (B).

Crosslinking density, p0, giving gel point in (A) is lower than that in (B) at the amount of two orders. Similar discussion is possible on the required crosslinking density giving a target of sol fraction.

When the target of sol fraction is 1 % for a polymer of P w = 2000, required crosslinkable units are 0.45 mol% in (A) and 9.5 mol% in (B). Much lower amount of crosslinkable units in (A), about onetwentieth of that in (B), can give the target of sol fraction.

According to the following analysis we can suggest the chemical structure of selfcrosslinkable acrylic dispersion Lakrytex 273, 430 (Fig. 5).

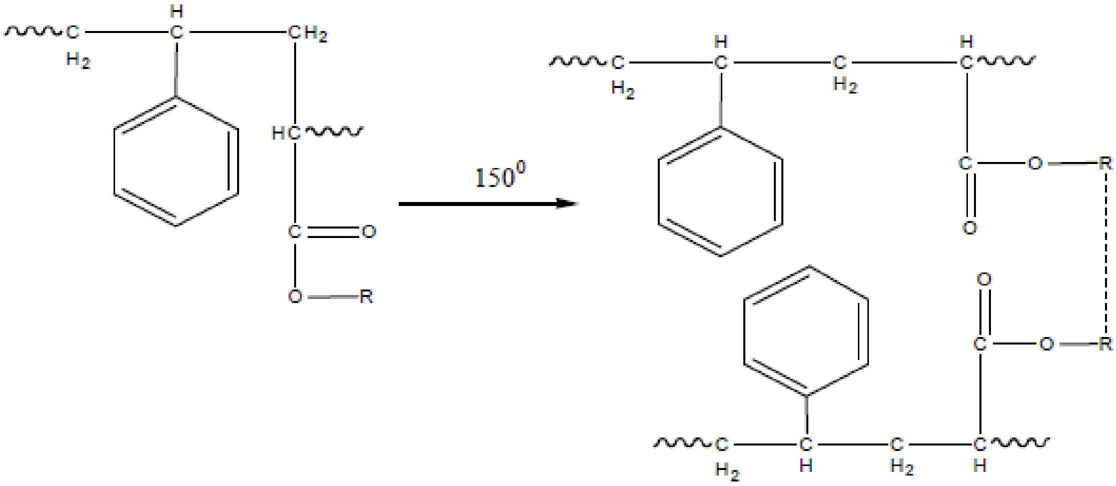

Fig. 5. Crosslinking of acrylic dispersions Lakrytex 273 and 430

As it`s shown (fig.5) crosslinked product is formed. In this case crosslinking is posable due to the mobile hydrogen atoms in the ends of monomer which are easily tiny and form new radicals by the reactions of crosslinking. With increasing the distance between the functional groups, the rate of crosslinking is growing [5].

Swelling data provides additional insights into the relationship between network and crosslinking density. This supports the theory that a higher initial double bond concentration produces a more densely crosslinked network.

Swelling studies were performed to investigate the degree of crosslinking and the degradation kinetics of the acrylates networks. The film samples were dissolved in water and the dissolution was monitored over time at room temperature using a simple gravimetric method. Four identical samples were prepared. The remaining crosslinked films were placed in 20 mL distillate water and were used for degradation and swelling studies. At selected time intervals, films were removed from solution and were patted dry and weighed to determine swollen mass (Ms). The films were then dried in oven and weighed to determine final dry mass (Mfd). The swelling degree of each film was calculated using the equation:

$$Sd = \frac{Ms - Mfd}{Mfd} \bullet 100$$

where Ms is the weight of the swollen film and Mfd is the weight of the final dried film.

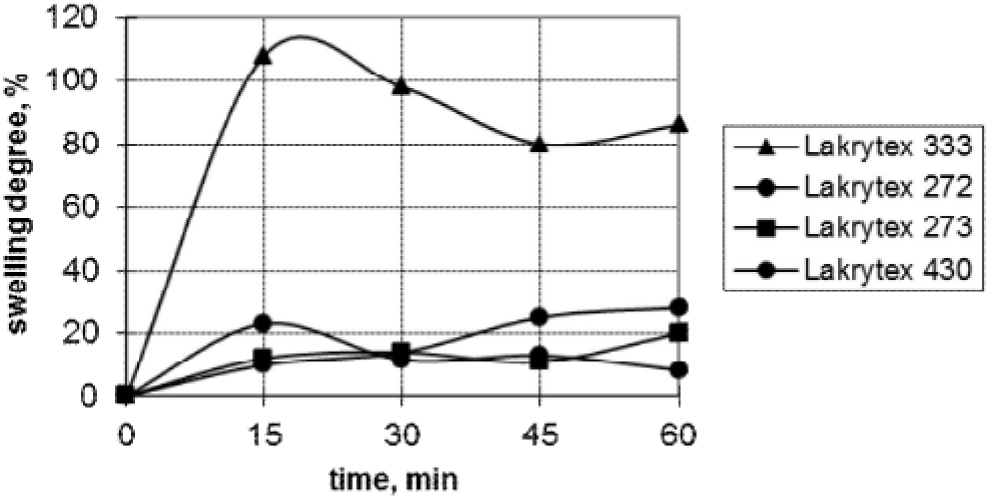

Fig. 6. The swelling kinetics of polymer films

As it described on the graph (fig. 6), films with a higher mass percentage of acrylates dissolved more slowly than those with a smaller amount of acrylate. This effect is explained by consideration of the crosslinking density in the formed films. In Lakrytex 273 the initial double bond concentration is higher therefore, the denser crosslinking sites, help to form tighter interpenetrating networks, resulting in slower dissolution rate due to the difficulty for water to penetrate the network.

Lakrytex 333 did not form stable crosslinked film under identical conditions, it have a high value of swelling degree so this justify that polymer didn't form crosslinking network and dissolve in solvents.

As Lakrytex 273 and 430 have a high crosslinking degree and didn't dissolve in solvents they have lower value of swelling degree.

A self-crosslinked film is formed, by a regular covalent bonds. The behavior depend on the tightness of the network; network such as shown in Figure 5 would exhibit less swelling than the network without crosslinked unites. Even with such models for an "ideal" homogeneous unimolecular network, however, a problem arises, for in many real cases the lengths of chains between crosslinks may vary depending on the structure of the monomers or prepolymers, or on the vagaries of reaction kinetics. Of particular interest to the next study of crosslinking is the influence of the effect of a distribution in the mass of the polymer film. Furthermore, a real polymer network is usually quite different from the ideal in structure. Not only do loops and dangling chain ends detract from the effectiveness of the structure, but shorter chains, either linear or branched, may exist without direct chemical connection to the network.

Introduced anhydride linkages in copolymers of styrene and ethyl acrylate, provides forming of crosslinked network. The ethyl acrylate is being used as a site for growth of crosslinks. Considering the chemical structure of self-crosslinkable acrylic copolymers networks can be assumed that the swelling ratio and the soluble fraction are decreased by increased crosslinking.

References

[1] Vincentz Verlag Self-crosslinking surfactant free acrylic dispersion // European coating journal 6/2001, pp. 2– 8

[2] Avvakumov N.I. Practicum on physics and chemistry of polymers / N.I. Avvakumov, L.A. Budarina, S.M. Dvigun – Moscow: Khimiya, 1990, pp. 193-195.

[3] Askadskii A.A. Computer-based Materiology of Polymers Vol. 1. Atomic and Molecular Line of Approach / A.A. Askadskii, V.I. Kondraschenko, – Moscow: Scientific World, 1999, p. 512

[4] Pasichnyk M., Slepchuk I., Michielsen S. Network characterization and swelling behavior of polymer composition for surface modification of textile materials // Science, Technology and Higher Education [Text] : materials of the

international research and practice conference, Westwood, Canada, December 11-12, 2012 / -c. Westwood, Canada, 2012. 472 – 485 p.

[5] Nikolaev A.F. Synthetic polymers and plastics on them. – Moscow: Chemistry, 1966. p. 768.

Network characterization and swelling behavior of polymer compositions

When self-linking in styrene-acrylic polymers takes place, not all carboxyl groups react. Therefore, admixtures of free acid monomers are deliberately added in industrial production of styrene-acrylic polymers to achieve maximum degree of interaction of the polymer with cross-linking agents.

Substances liable for the cross-linking actions of the macromolecules often contain the following groups:

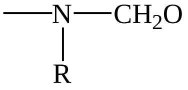

$-\underset{R}{N}-CH_2O$

- Methylol groups;

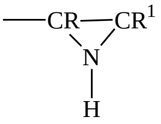

- Aziridine group;

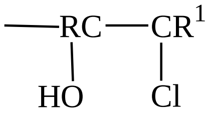

$-\underset{HO}{RC}-\underset{Cl}{CR^1}$

- Chlorohydroxy group;

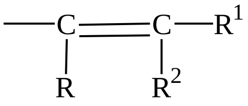

$-\underset{R}{C}=\underset{R^2}{C}-R^1$

- Compounds with double bonds;

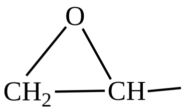

- Epoxy or glycidyl group

Substances capable of forming high cross-linked polymer film, are poly(oxypropylene)triol triglycidyl ether (TGE) based on the cross-linking reaction of glycidyl groups (Figure 7).and partially etherified melamine resin. In this case, interaction between the carboxyl groups of styrene-acrylic polymer and methylolene groups of the cross-linking agent is formed and a strong grid-type structure arises [35] (Fig. 8).

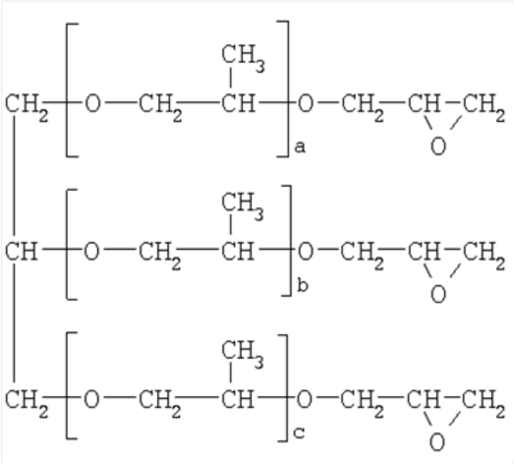

Fig. 7. The chemical structure of poly(oxypropylene)triol triglycidyl ether

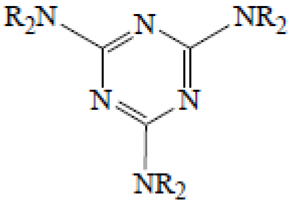

Fig. 8. Partially etherified melamine resin

R= -H, $-CH_2OH$, $-CH_2OCH_3$

The unique chemical structure of TGE molecule, the presence of three highly reactive glycidyl groups, can provide cross-linking reactions between polymer components and with the fiber-forming polymers [2].

The pronounced polar linkage of C - O in the epoxy cycle determines the ability of TGE to open the cycle under the action of nucleophilic and electrophilic reagents resulting in the formation of cross-linked polymers. The curing by the nucleophilic agents proceeds by the polycondensation mechanism or anionic polymerization. At the same time, the TGE has three reactive epoxy groups that can react with many compounds that contain reactive hydrogen atoms. Aside from the additive reactions, polymerization reactions are typical for TGE.

Epoxy groups can react with amines, phenols, mercaptans, isocyanates or acids. Amines are the most commonly used curing agents/hardeners for epoxides and the case of step - growth polymerizations is mainly represented by epoxy – amine reactions:

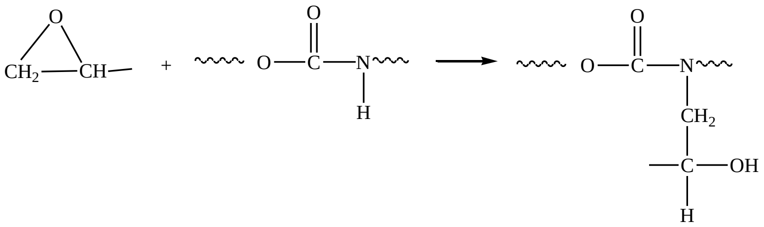

Usually when the concentration of epoxy groups is equal to or lower than the concentration of NH groups, side reactions do not take place. The epoxy – amine reaction is therefore suitable for the synthesis of “model” networks. The reactivity of the amine increases with its nucleophilic character:

aliphatic > cycloaliphatic > aromatic

Aliphatic amines are used for low - temperature curing systems (adhesives, coatings, etc.), and aromatic diamines for composite materials. Hydroxy groups catalyze the reaction through the formation of a trimolecular complex, which facilitates the nucleophilic attack of the amino group. As secondary alcohols are continuously generated, epoxy – amine reactions are autocatalyzed [3].

The glycidyl group is also capable of reacting with the terminal carboxyl groups of polymers:

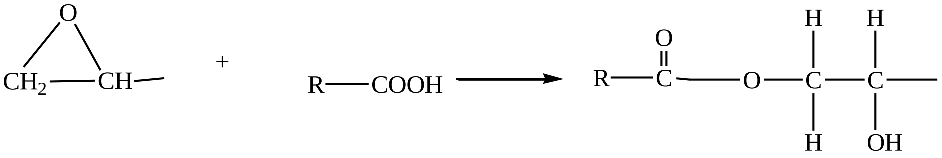

During interaction of epoxy groups with carboxyl groups, a sharp increase occurs in the density of the physical network (hydrogen bonds) due to appearance of hydroxyl groups.

The chemical reactions presented above suggest the possibility that the crosslinking agent is able to crosslink with polyurethane resin, which contains a secondary amino group and acrylic polymers with terminal carboxyl groups.

Since intermolecular cross bonds are formed by cross-linking, the linear or branched structures develop into three-dimensional polymer network that is unable to dissolve and melt. Therefore, the primary research method to determine the extent of polymer cross-linking is by equilibrium swelling or sol-gel analysis.

As a result of the experiment the film cast from polyurethane with the addition of hexamethylolmelamine dissolved during the extraction stage with acetone. We can make a conclusion that the formation of cross-links in polymer/crosslinking agent did not happen.

Table 2

Network characterization of polymer films

Cross-linking agent	Polymer dispersion	Sol fraction S, %	Cross-linking degree *j*,%	Fraction of active chains *Vc*	Swelling degree *a*, %	Fraction of moist-free polymer in the swollen gel *Vr*
Poly(oxypropylene)triol triglycidyl ether	PU	1,08	47	0,00036	6,1	1,7
	styrene-acrylic	1,8	32,4	0,12	6,45	0,15
Hexamethylolmelamine	PU	film is dissolved in solvents, the analysis is not possible				
	styrene-acrylic	7,1	10,24	29,19	4,6	3,47

The addition of three-functional glycidyl ether as a crosslinking agent to polymers provided the formation of cross-links between molecules, which prevents the separation of macromolecules and their run into the solvent.

In composition with three-functional glycidyl ether the highest degree of polyurethane resin crosslinking is 47%, besides the fraction of active chains in this composition is 0.0036, which indicates that cross-linking was complete.

The high degree of polyurethane polymers crosslinking using TGE can be explained by the interaction of amino groups of polyurethanes with epoxy groups as a result the three-dimensional structure forms:

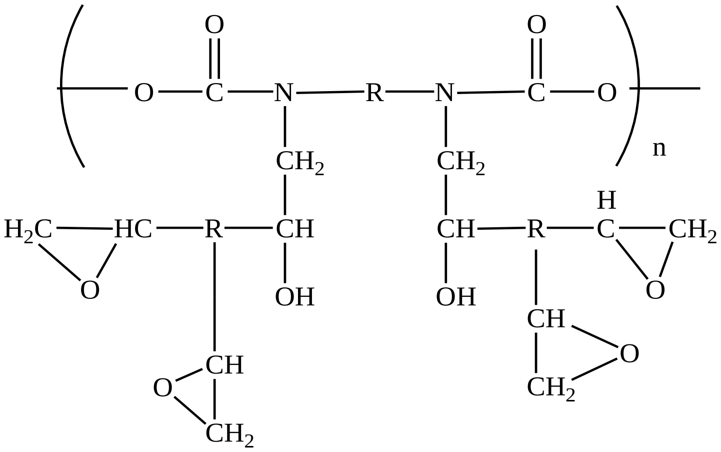

The chemical bond between carbon and nitrogen that occurs by cross-linking is resistant to most inorganic acids and alkalis. Hydroxyl groups formed by cross-linking are polar; it explains the low stability of the composition in organic acids and high stability in organic solvents. Free NH groups increase the resistance to non-polar solvents [5].

These figures are confirmed by infrared spectroscopy obtained during the study. There is no absorption in the region 915 cm^{-1} of IR spectrum that is responsible for the stretching vibrations of epoxy groups and the intensity of the band decreases at 3129 cm^{-1} that is responsible for amino group of polyurethane (fig. 9).

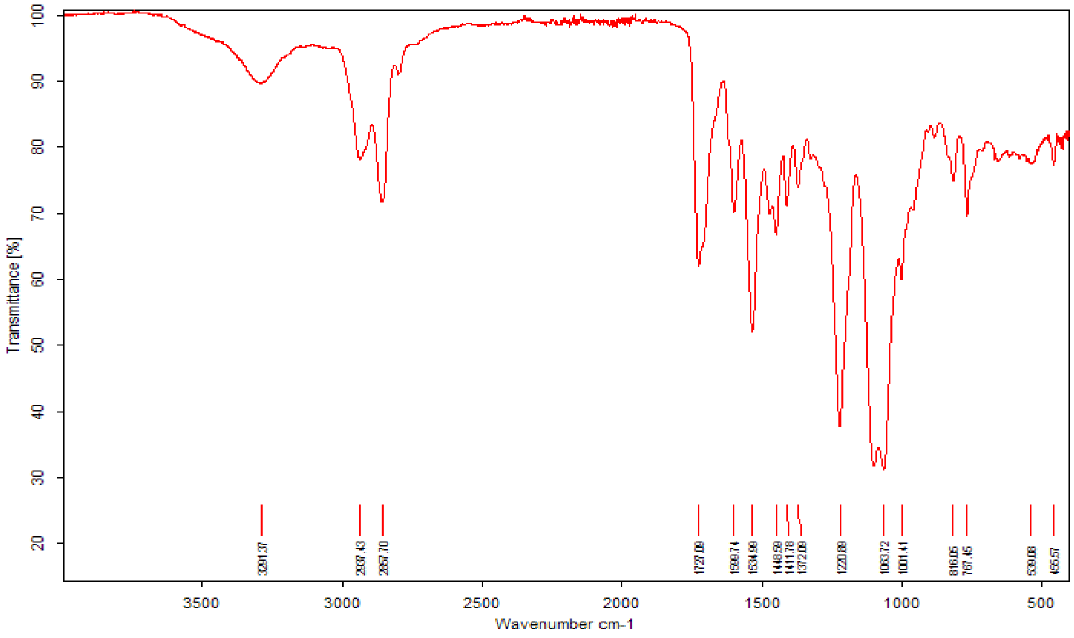

Fig. 9. Infrared spectroscopy of the film (polyurethane polymer crosslinking using TGE)

The high degree of styrene-acrylic polymer crosslinking with TGE provides interaction with the terminal carboxyl groups with epoxy. By the reaction of esterification the dense intermolecular packing forms:

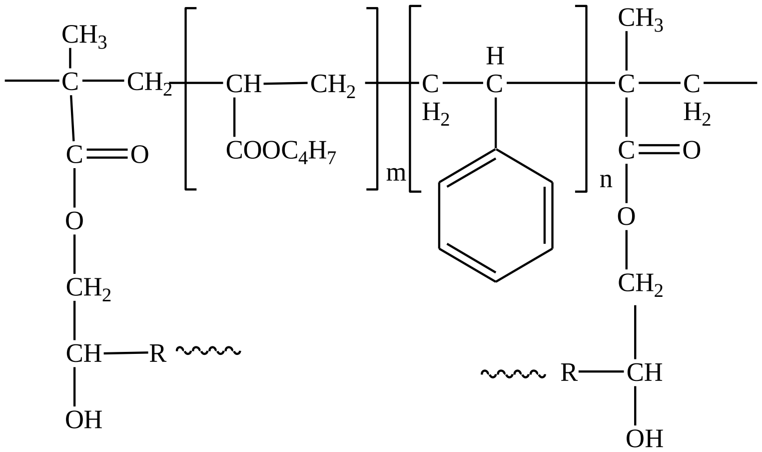

The interaction of epoxy groups with carboxyl leads to sharp increase in physical network density at the expense of hydroxyl groups introduction [6].

In data of IR spectra present an intense band at region 1151 cm^{-1} that is responsible for fluctuations esterified bonds (fig. 10).

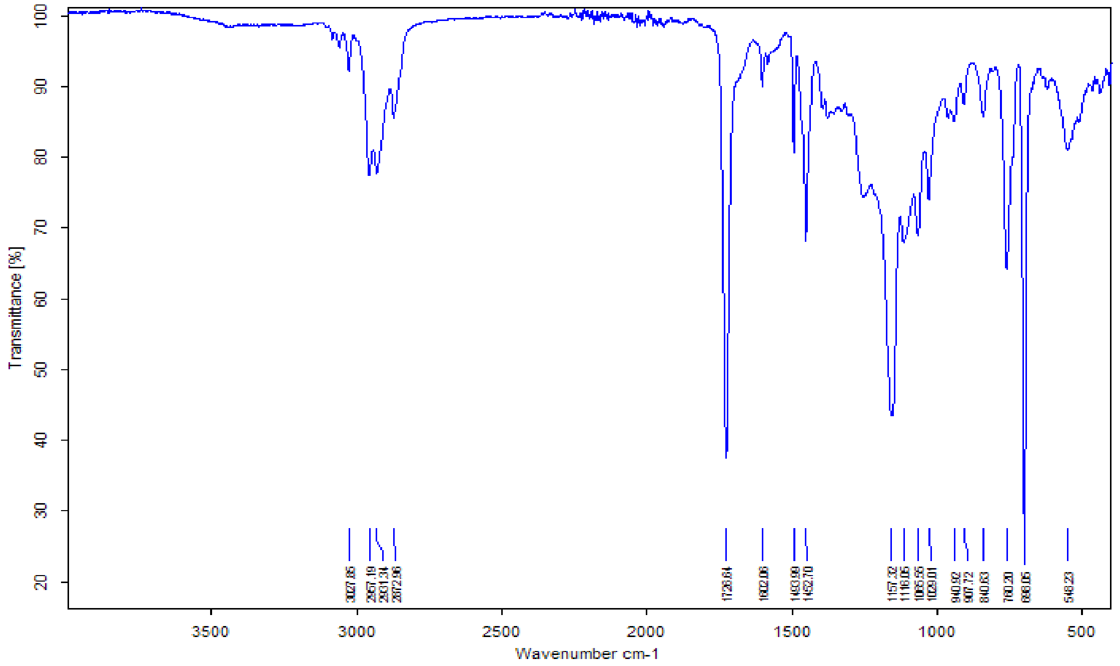

Fig. 10. Infrared spectroscopy of the film (styrene-acrylic polymer crosslinking using TGE)

The choice of TGE for three-dimensional cross-linked structure formation on the surface of textile material is justified by its unique chemical structure allows directionally modify the rheological, mechanical and relaxation properties of polymer materials.

At the same time TGE is an effective plasticizer which can significantly reduce the glass transition temperature of polymers and provide elasticity of the polymer formation.

Conclusions

Considering the chemical structure of polymers and cross-linking agents we can assume that the use of acrylic and polyurethane polymers with TGE can ensure the formation of a durable polymer coating with excellent adhesion due to cross-linking reactions TGEs glycidyl groups with the carboxyl groups of acrylic polymers, amine groups of polyurethane and hydroxyl groups of the fiber-forming polymer.

References:

1. Askadskii A.A. Computer-based Materiology of Polymers Vol. 1. Atomic and Molecular Line of Approach / A.A. Askadskii, V.I. Kondraschenko, – Moscow: Scientific World, 1999, p. 512
2. Pat. 2078094 of the Russian Federation, IPC C08G59/50, C09D163/00. Aliphatic ketimine glycidyl ethers of poly (oxypropylene) glycols and their methods of preparation / Gor'kov N.V, Lebedev V.S applicant and patentee Research and Production Enterprise Limited Liability Partnership "Macromer." - № 95106816/04, appl. 27/04/1995, publ. 27.04.1997, Bull. Number 2.
3. Pascault J.-P. Epoxy Polymers New Materials and Innovations / J.-P. Pascault, R. Williams – Weinheim: WILEY-VCH Verlag GmbH & Co. KGaA, 2010, 390 p.
4. Avvakumov N.I. Practicum on physics and chemistry of polymers / N.I. Avvakumov, L.A. Budarina, S.M. Dvigun – Moscow: Khimiya, 1990, pp. 193-195.

5. Prime R.B. Kinetics of Epoxy cure: 2. The System Bisphenol – A Diglycidyl Ether Polyamide / R.B. Prime // Polymer. – 1972. – №13, 455. – P. 45 – 48.
6. Grischuk O. Features of formation epoksiakrilat-urethane compositions in the presence of reactive liquid rubbers / O. Grischuk, A. Shevchuk, VV Shevchenko / / Polymer Journal. - 2004. - V. 26, № 3. - p. 196 - 200.

Synthesis of magnetite nanoparticles stabilized by polyvinylpyrrolidone and analysis of their absorption bands

The past decades saw active creation of new materials with decreased dimensionality. Among their diversity, we can separate magnetic nanomaterials.

Iron, nickel, cobalt, and oxides of these metals are normally used in order to obtain magnetic nanoparticles. The disadvantage of metals is that their magnetization decreases considerably at oxidation of the surface that is in contact with atmospheric oxygen. Magnetite Fe_3O_4 is devoid of this disadvantage [1]. The main advantages of magnetite include low susceptibility to oxidation, high magnetic properties, low cost, and significantly lower toxicity, unlike oxides of other metals [2].

The methods of chemical synthesis are used most often to control the size, shape, composition, structure, and physical properties of nanoparticles. By changing the dimensions, shape, composition and structure of nanoparticles, it is possible to control the magnetic characteristics within certain limits. The chemical method of co-sedimentation is the simplest and effective way of obtaining magnetic particles, the method was first described by Elmore [3], further his technique was modified by Massar [4].

Taking into account that the synthesis in aqueous medium is aimed primarily on preparation of magnetic dispersions of nanoparticles, one of the most effective and promising methods of stabilization was using different polyelectrolytes in the reaction mixture (that is *in situ*).

Control over processes of the synthesis of magnetite nanoparticles, selection of an appropriate stabilizer and analysis of its stabilizing action is a relevant task, because all this gives the opportunity to produce unique devices, based on magnetic nanoparticles, for various industries. Some of the most important requirements for such particles are non-toxicity, sedimentation, and chemical resistance [5]. In this regard, development of new ways for obtaining magnetite nanoparticles without the use of toxic reagents, such as oleates, trimethylamines or penthacarbonyls is a promising task.

Procedures of magnetite synthesis with the use of the method of co-sedimentation according to Elmor and Massar are currently employed increasingly often. For synthesis, solutions of ferrous salts are used in different ratios. For example, in paper [6], the process of co-sedimentation with solutions of salts of ferrum (II) chloride ($FeCl_2$) and ferrum (III) chloride ($FeCl_3$) with equal mole ratio of salts was carried out. 1 M solution of sodium hydroxide (NaOH) was used as a precipitant. As a result, particles with the radius of about 8 nm were formed. The main disadvantage of this method is duration of synthesis (4 hours), during which the magnetization of magnetite particles decreases considerably, moreover, they are devoid of their magnetic properties. In contrast to that research, scientists in article [7] used the same sedimentation agent, however, they replaced $FeCl_2$ with ferrum (II) sulfate ($FeSO_4$), and mole ratio of salts of Fe^{2+}/Fe^{3+} was 1:2. As a result of such synthesis, particles of dimensions in the range of 11–12 nm with highly pronounced magnetic properties were formed. However, the synthesis was conducted at low temperatures (about 0 ^{o}C), which required the use of additional refrigerants and greatly affected viscosity of the reaction mass. In article [8], the synthesis of salts $FeSO_4$ and $FeCl_3$ at mole ratio of 1:2 with the use of concentrated solution of ammonium hydroxide (NH_4OH) as a precipitant was carried out. The synthesis was performed in inert nitrogen medium. As a result, magnetite nanoparticles in the range from 4 to 17 nm with magnetic properties were formed. The advantage of this method over the other is a significant acceleration of the reaction, the synthesis lasted 30 min. The disadvantage is that the system is devoid of sedimentation stability and the process of synthesis should be carried out under rigid conditions at constant temperature control (70 °C). In such a system, there will be gradual oxidation of magnetite to ferrum (III) oxide and particulates will become larger.

An important issue for subsequent use of colloidal systems is stability of the system, which is getting particularly important in application of colloids. Therefore, stabilizers are added to create a potential barrier of repulsion of colloidal particles and to ensure aggregation resistance. Inorganic and organic substances, as well as synthetic and natural polymers can be used as stabilizers.

Thus, in paper [9], the magnetite particles (Fe_3O_4) were synthesized by the method of co-sedimentation with the use of sodium citrate (sodium salt of citric acid) and oleic acid as stabilizers. Phase composition and microstructure analysis indicate that sodium citrate and oleic acid were successfully grafted on the surface of Fe_3O_4, however, due to the surface effect, magnetization decreased considerably and the increased concentration of stabilizers led to a significant decrease in crystallinity of the resulting oxide. Formation of polysaccharide coating on the nanomagnetite surface also prevents aggregation of particles [10]. The advantages of using polysaccharides is that most of them are non-toxic substances, the downside is that their molecules can be desorbed from the surface of ferrous oxide by heating up to 120^0 C or dilution, which considerably decreases the scope of application of the resulting colloids.

PVP was used as a stabilizer during synthesis of nanoparticles of silver. Scientists found that PVP acts as a surface stabilizer, a modifier of an increase in nanoparticles and a disperser [11]. It has protective properties due to its unique structure (Fig. 11) [12].

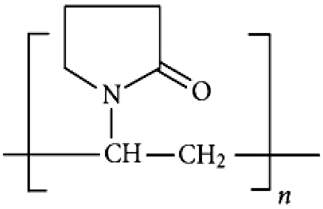

Fig. 11. Formula of polyvinylpyrrolidone

A molecule contains a highly polar amide group, which provides hydrophilic properties, as well as non-polar methyl groups both in the skeleton and in the ring, which provide hydrophobic properties. In addition, it is a non-toxic, biocompatible substance. However, in this work, the PVP were applied using the method of post-synthetic coating, which involved application of the polymer to the surface of nanoparticles that have already been synthesized. This method considerably complicates the process of synthesis since it requires strict control over all components of the reaction. In addition, the method of post-synthetic coating leads to passivation of the active surface of nanoparticles, which is not appropriate for magnetite nanoparticles.

Critical analysis proved that there is no universal technique for the synthesis of magnetite nanoparticles. The use of the method for co-sedimentation using ferrum Fe^{2+}/Fe^{3+} in a certain ratio as salts requires optimization and selection of the required concentrations of reagents and the reacting substances. It is advisable to carry out the synthesis in the solution of a stabilizer, rather than add it after the co-sedimentation process to increase stability of the resulting dispersions. In this way, the time spent on synthesis will be saved, in addition, formation of stable particles of certain dimensions is possible during the synthesis, since a stabilizer will resist aggregation and enlargement of the particles at the nucleation stage. All these assumptions require thorough research and proving.

The aim of this work was to develop a procedure for obtaining magnetite nanoparticles using polyvinylpyrrolidone (PVP 3.5 %) as a dispersed medium, and to study the spectra of optical absorption of the resulting nanomagnetite dispersions with the help of the spectrophotometric method of analysis.

To accomplish the aim, the following tasks have been set:

– to select working concentrations of the reacting substances and to perform synthesis of magnetite nanoparticles using PVP (3.5 %) as a dispersed medium;

– using the method of spectrophotometry, to obtain the bands of absorption of aqueous dispersions of nanomagnetite and analyze them using the theory of plasmon oscillations;

– using the method of spectrophotometry, to get the bands of absorption of nanomagnetite dispersions using 3.5 % PVP as the dispersed medium and to analyze them using the theory of plasmon oscillations;

– to propose a possible mechanism of stabilization of magnetite nanoparticles with polyvinylpyrrolidone.

In work, the following chemical reagents were used for the synthesis of magnetite: ferrum (II) sulfate heptahydrate ($FeSO_4 \cdot 7H_2O$) – "chemically pure" GOST 4148-66, ferrum (III) chloride hexahydrate ($FeCl_3 \cdot 6H_2O$) – "chemically pure" GOST 4147–74, 25 % water solution of ammoniac (NH_4OH) "chemically pure" GOST 3760–64. The synthesis was carried out separately in water and separately in aqueous solution of PVP of 3.5 % concentration, with average molecular weight of $3 \cdot 10^4$.

Procedure for the synthesis of magnetite nanoparticles

To carry out the reaction, the batch of $FeSO_4 \cdot 7H_2O$ and the batch of $FeCl_3 \cdot 6H_2O$ were dissolved in 100 ml of water and in 100 ml of PVP (3.5 %). Then the solutions were filtered to remove insoluble residues of salts. After that, the solutions were stirred with a magnetic stirrer. Concentrated ammoniac solution (25 %) was added to solution of ferrous salts at the rate of one drop per second.

The process can be represented as the following chemical equation:

$$Fe^{2+} + 2Fe^{3+} + 8OH^{-} = Fe_3O_4 + 4H_2O. \qquad (1)$$

Determining main parameters of the nanoparticles synthesized in an aqueous solution

Sedimentation constant K can be calculated from formula:

$$K = \sqrt{\frac{9\eta}{2g(\rho - \rho_0)}}, \qquad (2)$$

where ρ is the density, kg/m^3; g is the gravitational acceleration, m/s²; η is the viscosity of the medium, Pa·s.

Sedimentation constant K is a constant magnitude for the given system, which is why the particle's radius was calculated from formula:

$$r = K\sqrt{\frac{H}{\tau}}, \tag{3}$$

where K is the sedimentation constant, H is the height, mm, τ is the time, necessary for a particle to reach the bottom of a vessel, s.

The motion velocity of a particle relative to the medium, in which a particle is weighed, was determined from formula:

$$u = \frac{2\Delta\rho g m^2}{9\eta}, \tag{4}$$

where ρ is the density, kg/m^3; g is the gravitation acceleration, м/s²; η is the viscosity of the medium, Pa·s, the weight of a particle, g.

The weight of a particle was determined from formula:

$$m = V \cdot \rho = \frac{4}{3}\pi \cdot r^3 \cdot \rho. \tag{5}$$

From formula (2), it is possible to estimate the time of sedimentation of dispersion ts as the time, necessary for particles to pass the path that is equal to the height of the vessel H:

$$t_s = \frac{H}{u}. \tag{6}$$

Procedure for determining the spectral characteristics of dispersions

Spectra of absorption of magnetite nanoparticles solutions in water and in 3.5 % PVP were registered by spectrophotometer SF-56 in quartz drainage ditch with the length of the absorbing layer of 10 mm in the range of 200–800 nm for aqueous solutions and the range of 190–1,110 for dispersions in 3.5 % of PVP.

Results of synthesis of magnetite nanoparticles with the use of 3.5 % PVP as dispersed medium and analysis of spectra of optical absorption of resulting dispersions taken with the use of the spectrophotometric method

1. Selection of operating concentrations of reacting substances and performing synthesis of magnetite nanoparticles

Salts of ferrum (II) sulfate and ferrum (III) chloride and concentrated aqueous ammoniac solution were used for co-sedimentation in the study. Most of the sources recommend to perform interaction at the mole ratio of salts of iron Fe^{2+}/Fe^{3} equal to 1:2, at the same time, the concentration of salts and the added base differ significantly. In this regard, the first stage of the study was aimed at the selection of operating concentrations of salts and ammoniac and sedimentation took place in the aqueous solution. There were 5 preparations of magnetic particles, in the process of synthesis of which solution of 7.5–0.25 % by weight of ferrous salts (final concentration) was used, to which concentrated ammoniac solution was added (Table 1).

Table 3

Main characteristics of synthesized solutions

No. by r	NH_4OH, %	Concentration (Fe^{2+}/Fe^{3+}), %	Sedimentation rate, m/s	Radius of particles, nm	Weight of particles, g
1	25.0	7.5	$5 \cdot 10^{-1}$	70	$1.5 \cdot 10^{6}$
2	12.5	3.8	$1 \cdot 10^{-1}$	55	$7.8 \cdot 10^{4}$
3	3.5	1.0	$2.5 \cdot 10^{-3}$	20	$2.1 \cdot 10^{3}$
4	2.0	0.5	$2.0 \cdot 10^{-3}$	8	2.7
5	1.5	0.3	$1.0 \cdot 10^{-4}$	4	0.1

In the course of the experiment it was found that the excess of ammoniac solution leads to unstable dispersions. The most stable, and thus the least aggregated particles were obtained by adding 1.5–2.0 % ammoniac at concentration of ferrous salts of 0.5–0.3 %, respectively. In this case, the ratio of Fe^{2+}/Fe^{3+} was not 1:2, as most researchers have, but was on average 1.0:1.5. At such ratio of salts, there were formed black dispersions of magnetite nanoparticles of the radius of 4–8 nm with magnetic properties that were checked by carrying the dispersions into the magnetic field (magnetite nanoparticles were attracted to a magnet). High concentrations of ferrous salts do not form dispersions with magnetic properties, such dispersions are grayish brown, the formed particles are non-homogeneous, the average radius of them is 55–70 nm.

Next, to conduct synthesis of magnetite particles with the use of PVP (3.5 %) as dispersed medium, the concentration of ferrous salts Fe^{2+}/Fe^{3} 0.5–0.3 % was selected and the amount of the added ammoniac was within 1.5–2.0 %. At the first stage of the synthesis, selected concentration of ferrous salts Fe^{2+}/Fe^{3} was dissolved in 100 ml of 3.5 % PVP. At the second stage, the solution with ferrous salts was stirred with a magnetic stirrer and the required volume of concentrated ammoniac solution was added at the rate of one drop per minute.

As a result of the synthesis, aggregation resistant dispersion of magnetite nanoparticles of black color was formed.

The dimensions of nanoparticles and chemical composition of the dispersed medium affect the main spectral characteristics of the formed solutions, which helped analyze the major changes that occur in the electronic structure of synthesized particles. Therefore, based on the ideas of plasmon resonance, the spectrophotometry method with further analysis of the bands of optical absorption of dispersions was used for the characteristic of the synthesized nanoparticles [13].

2. Analysis of spectral characteristics of the formed dispersions

Nowadays, when analyzing metallic nanoparticles, the dimensions of which are smaller or similar to the depth of penetration of electromagnetic wave in metal, increased attention is paid to the study of surface plasmon resonance [14].

For magnetite nanoparticles, synthesized in aqueous solution based on measurement of absorption spectra, existence of a peak at wave length of 350 nm was shown (Fig. 2, 3). Light absorption occurs in close ultraviolet, this absorption is associated with appearance of the surface plasmon resonance on the nanoparticle’s surface. Electronic density of the layer in magnetite nanoparticles is much higher than in typical plasmons, respectively, for transition of electrons from the d to s^2 sub-level, it is necessary to spend less energy. As a result of absorption at 350 nm, it is formed due to transition of electrons from one *d* orbital to another and by transfer of electrons from anion to cation in Fe_3O_4. That is, there is a shift of the central metal ion that forms a strong covalent bond with the surrounding oxygen ions, using its empty *d* orbital.

A significant decrease in concentration of reacting substances in the synthesis of nanoparticles affects the position of the absorption band, which is characterized by maximum at 350 nm. As a result of high concentrations of reacting substances (concentration of salts of Fe^{2+}/Fe^{3+} is 7.5–1.0 %; concentration of ammoniac is 25–3.5 %), synthesized nanoparticles are characterized by large dimensions of 55–70 nm and a high aggregation degree (Fig. 2, sample 3). Due to electrodynamic interaction between closely spaced nanoparticles, the spectral state of plasmon resonance changes [15]. Dense packing of nanoparticles results in formation of collective plasmon resonance [16]. The result of manifestation of strong lateral interactions in a densely-packed mono-layer is a considerable long-wave shift of the maximum of the absorption band from 300 nm to 380 nm (bathochromic shift by 80 nm). The formed shoulder indicates a totality of partially aggregated particles (Fig. 11, sample 1, sample 2).

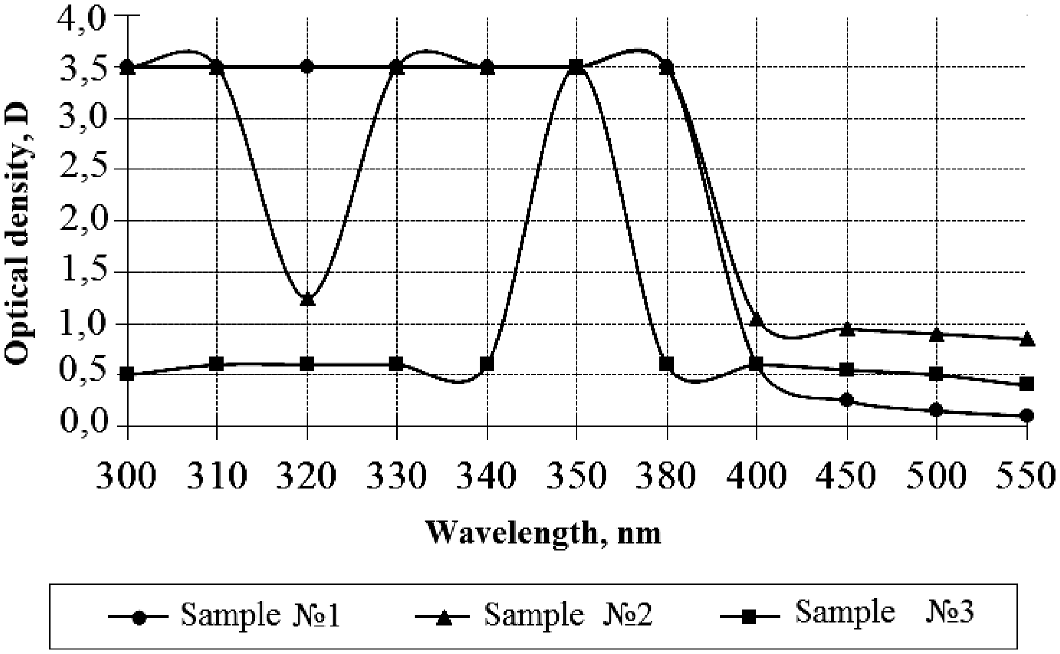

Fig. 12. Spectra of absorption of solutions of magnetite nanoparticles, synthesized in aqueous medium (length of absorbing layer is 10 mm). Sample 1: concentration of salts of Fe^{2+}/Fe^{3+} is 7.5 %, ammoniac concentration is 25 %. Sample 2: concentration of salts of Fe^{2+}/Fe^{3+} is 3.8 %, ammoniac concentration is 12.5 %. Sample 3: concentration of salts of Fe^{2+}/Fe^{3+} is 1.0 %, ammoniac concentration is 3.5 %

Fig. 13 shows the spectra of absorption of fluids with low concentrations of reacting substances (concentration of salts of Fe^{2+}/Fe^{3+} is 0.5–0.3 %; ammoniac concentration is 1.5–2.0 %). As Fig. 2 shows, the shift of absorption band did not occur, however the value of optical density is different. The highest D=0.8 is for sample 4, the lowest D=0.25 is for standard 5. Absorption maximum in all solutions is at 350 nm. The frequency of the band decreases, a hypochromic band shift by 30 nm with the hypochromic effect by 80 % for sample 4 and by 93 % for sample 5.

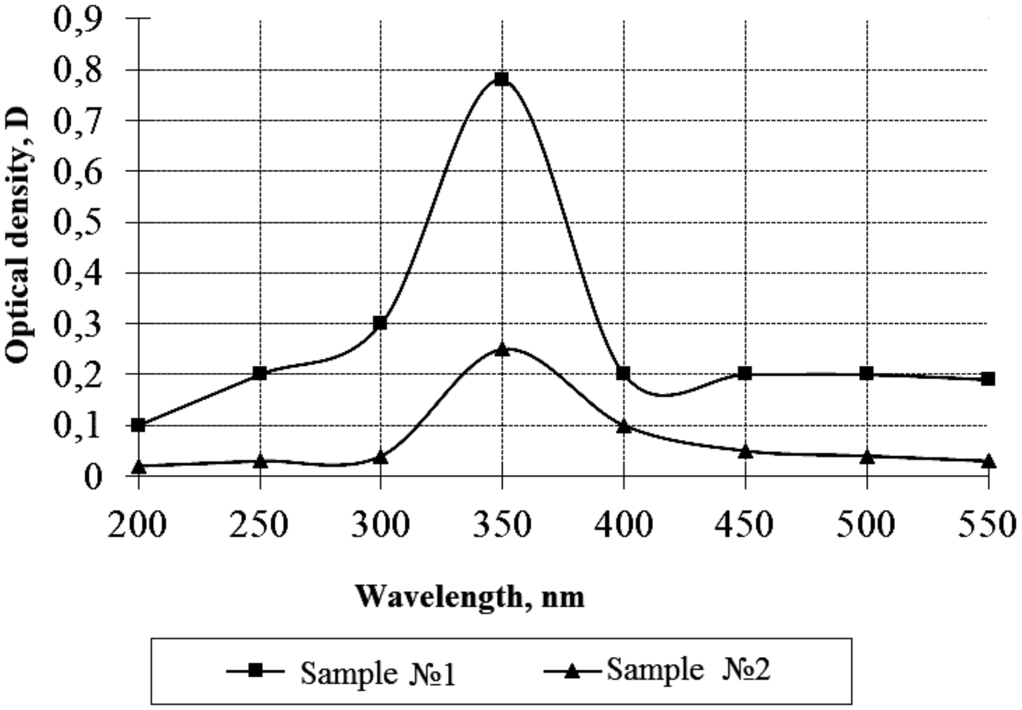

Fig. 13. Spectra of absorption of solutions of magnetite particles, synthesized in aqueous medium (the length of the absorption layer is 10 mm). Sample 4:

concentration of salts of Fe^{2+}/Fe^{3+} is 0.5 %, ammoniac concentration is 2.0 %. Sample 5: concentration of salts of Fe^{2+}/Fe^{3+} is 0.3 %, ammoniac concentration is 1.5 %

As Fig. 12, 13 show, high concentrations of reacting substances (concentration of salts of Fe^{2+}/Fe^{3+} is 7.5–1.0 %; ammoniac concentration is 25–3.5 %) characterize the changes in absorption spectra as hyperchromic effect, whereas low concentrations of reacting substances (concentration of salts of Fe^{2+}/Fe^{3+} is 0.5–0.3 %; ammoniac concentration is 1.5–2.0 %) characterize spectral changes by hypochromic effect.

Absorption spectra of magnetite nanoparticles, synthesized using 3.5 % PVP as dispersed medium, are shown in Fig. 14. An intense absorption band appears on the spectrum at 950 nm. Absorption peak shifts toward longer wavelengths due to a decrease in dimensions of nanoparticles. The absorption band is characterized by existence of three peaks at 350 nm, 950 nm and 1,050 nm. Existence of several absorption peaks indicates that in the presence of PVP, the co-sedimentation reaction occurs stage by stage. First, there is a process of rapid nucleation, which corresponds to the value of the peak at λ=350 nm, then concentration of the substance reaches the critical over-saturation, which is proved by disappearance of the peaks to λ=950 nm. At the given wavelength, there occurs a slow nucleus growth by diffusion of the PVP chains to the nanomagnetite surface.

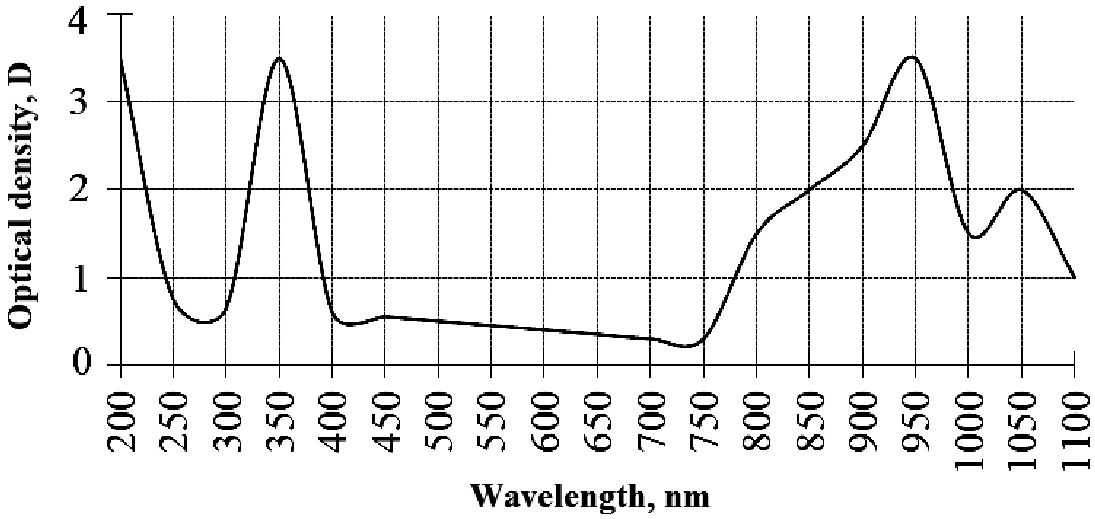

Fig. 14. Spectrum of absorption of dispersion of magnetite nanopartiles, synthesized with the use of 3.5 % polyvinylpyrrolidone *M*(PVP) $3 \cdot 10^4$ as dispersed medium. The length of the absorption layer is 10 mm. Concentration of salts of Fe^{2+}/Fe^{3+} is 0.5 %; ammoniac concentration is 2.0 %

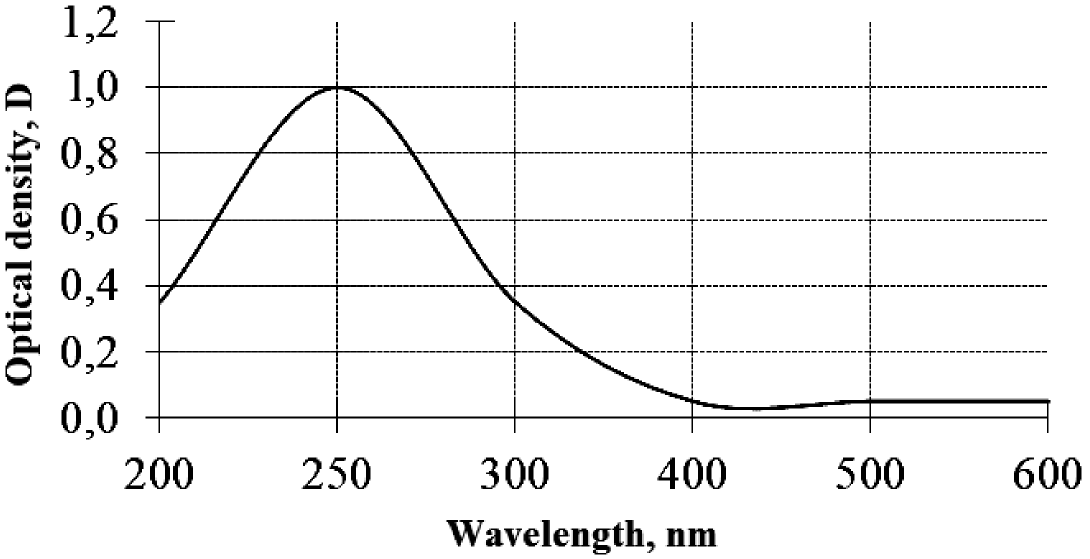

Fig. 15. Spectrum of absorption of 3.5 % solution of polyvinylpyrrolidone *M* (PVP) $3 \cdot 10^4$, the length of absorbing layer is 10 mm

As Fig. 15 shows, the absorption band of 3.5 % PVP has a maximum at 250 nm, which corresponds to absorption of the solution slurry in close ultraviolet, the absorption band is weak $\varepsilon<10^2$ transition $n \rightarrow \pi^*$. Disappearance of the band at 250 nm shows that formation of a coordinating bond between PVP and magnetite at the expense of free electrons of oxygen and nitrogen occurred (Fig. 16):

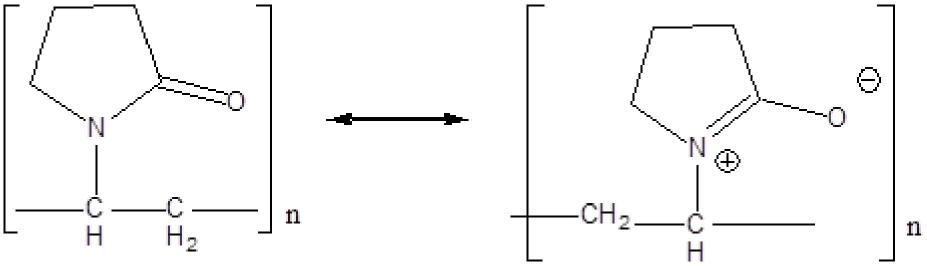

Fig. 16. Schematic of polyvinylpyrrolidone regrouping into molecules

The existence of a peak at 350 nm indicates formation of magnetite nanoparticles. Magnetite nanoparticles interact with PVP, the bathochromic shift with a maximum at 950 nm appears on the spectrum (Fig. 14).

Sensitivity of plasmon absorption resonances is due to the interaction of the magnetite electrons with π-electrons of PVP [17] (Fig. 17).

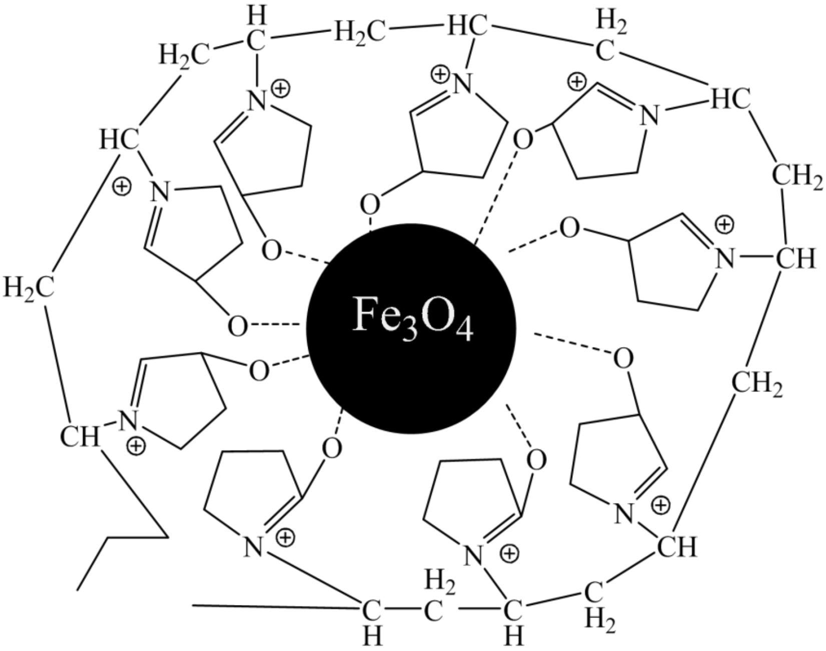

Fig. 17. Schematic representation of magnetite nanoparticles' stabilization by polyvinylpyrrolidone

During synthesis of magnetite nanoparticles with the use of 3.5 % PVP as dispersed medium, most atoms of metal contact with the surface of the polymer. As a result of the interaction, greater number of magnetite electrons is able to interact actively with π-electrons of PVP in the process of nanoparticles formation. Dimensions of synthesized nanoparticles significantly decrease, which is proved by existence of peaks in the absorption spectrum at λ=950 nm and at λ=1050 nm.

Polyvinyl groups have significant repulsive power [18], taking into account the large molecular mass of the polymer, the phenomenon of steric obstacle occurs (Fig. 18).

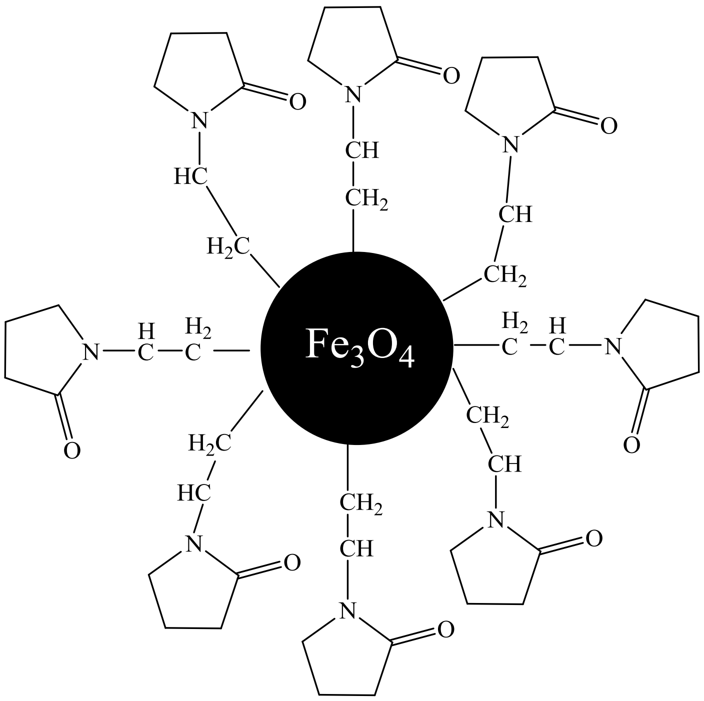

Fig. 18. Schematic representation of magnetite nanoparticles' stabilization by polyvinylpyrrolidone

Let us assume that the stabilization mechanism is associated with the possibility of PVP to spread in a limited way, thus forming short polymer chains, which are able to be absorbed on the surface of magnetite and prevent aggregation of nanoparticles.

The approach that combines synthesis and modification of magnetite nanoparticles was proposed, as a result, aggregation resistant dispersions of nanoparticles with sedimentation rate of $2.0 \cdot 10^{-3}$–$1.0 \cdot 10^{-4}$ m/s are formed. Non-toxic 3.5 % PVP is used as a stabilizer. During this synthesis, particles with the radius of

4– 8 nm are formed. It was shown that to resist aggregation of magnetite nanoparticles and for synthesis of nanoparticles with a small distribution by dimensions, it is advisable to carry out the synthesis with the use of 3.5 % PVP as dispersed medium. Currently, this research is relevant, because in the work, the spectra of optical absorption of resulting dispersions of nanomagnetite were studied with the help of the spectrophotometric method.

A significant simplification and acceleration of the process of synthesis of magnetite nanoparticles compared with the known research [6–9] was shown. Thus, in contrast to papers [6–9], it was possible to decrease the duration of synthesis from 4 hours to 2 minutes. The process of synthesis was carried out without the use of refrigerants, without constant passing nitrogen and without rigid temperature control of the system. It was determined that the concentration of 2:1 of ferrous salts, proposed in [7], is not advisable, and at a decrease in the ratio of ferrous salts to 1.5:1.0, magnetite particles are also formed, in this case, reagents are saved. The optimal way of introducing the reagent, which was not described in previous works, was proposed. Thus, for example, during simultaneous introduction of all components (direct pouring), magnetite oxidation to Fe_2O_3 is possible, particles get larger, the system loses aggregation resistance, and the process should be carried out at low temperatures [8]. In this study it was found that a parallel way of reagents' introduction is the most appropriate. In the proposed synthesis, the rate of ammoniac introduction is one drop per minute at constant stirring of the reaction mixture, in this case, the reaction goes at high rate.

It was found that an increase in concentration and volume of a reducing agent leads to formation of particles of large radius of 70 nm. Thus, at high concentrations of reacting substances (Fe^{2+}/Fe^{3+} – 7.5–1,0 %; NH_4OH – 25–3.5 %), dispersions with particles of 55–70 nm, which are characterized by weak magnetic properties (not attracted to a magnet) and have grayish-brown-black color, which indirectly indicates that the particles contain impurities of goethite (FeO (OH)). The most aggregation resistant dispersions are produced during a short time of hydrolysis (up to 2 minutes) after adding ammoniac and a change of concentration of salts of ferrum

Fe^{2+}/Fe^{3+} in the ratio of 1.0–1.5. Under such conditions and at such ratio of the components, magnetite with the average radius of 4–8 nm was obtained.

Analysis of the absorption bands of the formed dispersions showed that at the change in dimensions of nanoparticles, there is no change of a spectral shift of the plasmon absorption band, but there is a change in its amplitude. At a subsequent change of dimensions of nanoparticles from 70 nm to 8 nm, a two-wave shift of the plasmon band by 30 nm and a decrease in its amplitude by 80 % occur.

The conducted studies of the surface plasmon resonance of the synthesized solutions made it possible to establish existence of the absorption peak at 350 nm in all aqueous dispersions of nanomagnetite. The nature and intensity of absorption bands depend on the concentration of reacting substances and the method of reagents' introduction (direct introduction or parallel introduction of reagents). Intensity of weak absorption bands is determined mainly by d–p shift, i.e. the transition of electrons d→d in some degree takes on the character of transitions p→d, which occur between ions in magnetite.

During the synthesis of magnetite nanoparticles in 3.5 % PVP, dispersion of free electrons on the surface of a particle occurs, so plasmon frequency of free oscillations of electrons is shifted from the ultraviolet to the visible region of the spectrum. Analysis of absorption bands of nanoparticles, synthesized in 3.5 % PVP, showed existence of 3 absorption waves at λ=350 nm, λ=950 nm and λ=1,050 nm. The existence of several absorption bands indicates that in the presence of PVP, a co-sedimentation reaction occurs stage by stage, first there is a process of rapid nucleation, and then, there is a slow nucleus growth through diffusion of the PVP chains to the surface of nanoparticles. Accordingly, these two stages should be separated for the controlled synthesis of magnetite nanoparticles, and nucleation should be avoided during the growth of nanoparticles. In such a case, particles with dimensions in the nanometer range will be synthesized, and formed dispersions will be characterized by aggregation resistance and stability, which will significantly expand the scope of application of the formed nanocolloids in medicine for addressed delivery of medicines, in the textile industry for finishing of textile materials, in the chemical industry for wastewater treatment, etc.

The spectrophotometric method, which was used in the study (SF-56), make it possible to register the indicators in the visible and ultraviolet region of the spectrum (190–1200 nm), which is the main limitation of this study. The minimum value of optical density, which can be measured using SF 56 with necessary precision, is typically equal to 0.01, and the thickness of the layer is on average 1 cm. The minimum value of the concentrations, which is determined on SF-56, is approximately 10^{-7} M (10^{-2} μg/ml or mg/l). Therefore, when working with SF-56, it is necessary to ensure selectivity mostly at the stage of sampling through selection of reagents, as well as by conditions of determining (pH variation and choice of a solvent).

In the further research, it would be advisable to combine this method with translucent electron microscopy in order to establish the relationship between the morphology of the formed nanoparticles and their plasmon absorption bands.

Conclusions

1. In the course of the study, it was found that particles with the smallest radius of 4–8 nm were formed at concentrations of salts of ferrum Fe^{2+}/Fe^{3+} of 1.0:1.5 respectively, and the amount of added ammoniac was 2.0 %. The character of reagents' introduction was parallel, the rate of ammoniac introduction was one drop per minute at constant stirring of the reaction mixture.

2. An analysis of the absorption bands of the nanoparticles, synthesized in aqueous solution, showed that the resulting dispersions are characterized by a peak at 350 nm. The dimensions, weight and radius of the nanoparticles affect the character of absorption bands. Thus, high concentrations (Fe^{2+}/Fe^{3+} is 7.5–1.0 %; NH_4OH is 25–3.5 %) of the reacting substances lead to formation of large particles of 70 nm, which create agglomerates and shift the absorption band in a bathochromic way by 30 nm. Low concentrations of the reacting substances (Fe^{2+}/Fe^{3+} is 0.5–0.3 %; NH_4OH is 1.5–2.0 %) lead to formation of more stable, lower in size particles

of 4–8 nm, and the resulting solutions are characterized by a distinct absorption band at 350 nm.

3. Analysis of bands of absorption of solutions of magnetite nanoparticles, synthesized with the use of 3.5 % PVP as dispersed medium, showed existence of 3 absorption strips at λ=350 nm, λ=950 nm and λ=1050 nm. A band at 350 nm indicates formation of magnetite nanoparticles. At 250 nm, the band that is typical of valence fluctuations of PVP disappears on the spectrum. The bathochromic shift by 600 nm occurs in the system. The absorption band is quite intense and typical of transitions of electrons from π orbital in the conjugated system.

4. The mechanism of stabilization of nanomagnetite PVP occurs due to the interaction of magnetite electrons with π-electrons of PVP in the process of nanoparticles formation. At the first stage of the process of synthesis, magnetite nanoparticles are formed, which is proved by the existence of a peak of the absorption band at 350 nm. At the second stage, partial adsorption of PVP chains to the surface of magnetite nanoparticles occurs, which is proved by disappearance of the absorption band at 250 nm.

References

1. Faraji M., Yamini Y., Rezaee M. Magnetic nanoparticles: Synthesis, stabilization, functionalization, characterization, and applications // Journal of the Iranian Chemical Society. 2010. Vol. 7, Issue 1. P. 1–37. doi: 10.1007/bf03245856

2. Superparamagnetic iron oxide: pharmacokinetics and toxicity / Weissleder R., Stark D., Engelstad B., Bacon B., Compton C., White D. et. al. // American Journal of Roentgenology. 1989. Vol. 152, Issue 1. P. 167–173. doi: 10.2214/ajr.152.1.167

3. Elmore W. C. Ferromagnetic Colloid for Studying Magnetic Structures // Physical Review. 1938. Vol. 54, Issue 4. P. 309–310. doi: 10.1103/physrev.54.309

4. Massart R. Preparation of aqueous magnetic liquids in alkaline and acidic media // IEEE Transactions on Magnetics. 1981. Vol. 17, Issue 2. P. 1247–1248. doi: 10.1109/tmag.1981.1061188

5. Baranov D. A., Gubin S. P. Magnitnye nanochasticy: dostizheniya i problemy himicheskogo sinteza // Nanosistemy. 2009. Vol. 1, Issue 1-2. P. 129–147.

6. Dynamic magnetic behaviour and Mössbauer effect measurements of magnetite nanoparticles prepared by a new technique in the co-precipitation method / Bandhu A., Mukherjee S., Acharya S., Modak S., Brahma S. K., Das D., Chakrabarti P. K. // Solid State Communications. 2009. Vol. 149, Issue 41-42. P. 1790–1794. doi: 10.1016/j.ssc.2009.07.018

7. Novel mechanochemical process for synthesis of magnetite nanoparticles using coprecipitation method / Iwasaki T., Kosaka K., Yabuuchi T., Watano S., Yanagida T., Kawai T. // Advanced Powder Technology. 2009. Vol. 20, Issue 6. P. 521–528. doi: 10.1016/j.apt.2009.06.002

8. Directly aqueous synthesis of well-dispersed superparamagnetic Fe3O4 nanoparticles using ionic liquid-assisted co-precipitation method / Hu J., Hu X., Chen A., Zhao S. // Journal of Alloys and Compounds. 2014. Vol. 603. P. 1–6. doi: 10.1016/j.jallcom.2014.02.022

9. Synthesis of Fe3O4 Nanoparticles and their Magnetic Properties / Wei Y., Han B., Hu X., Lin Y., Wang X., Deng X. // Procedia Engineering. 2012. Vol. 27. P. 632–637. doi: 10.1016/j.proeng.2011.12.498

10. Synthesis and characterization of Fe3O4 nanoparticles coated with fucan polysaccharides / Silva V. A. J., Andrade P. L., Silva M. P. C., Bustamante D., A., De Los Santos Valladares L., Albino Aguiar J. // Journal of Magnetism and Magnetic Materials. 2013. Vol. 343. P. 138–143. doi: 10.1016/j.jmmm.2013.04.062

11. Osoblyvosti oderzhannia nanochastynok sribla u prysutnosti polivinilpirolidonu / Semeniuk N. B., Kostiv U. V., Dziaman I. Z., Klym Yu. V., Skorokhoda V. Y. // Visnyk Natsionalnoho universytetu "Lvivska politekhnika". Ser.: Khimiya, tekhnolohiya rechovyn ta yikh zastosuvannia. 2014. Issue 787. P. 440–443. URL: http://nbuv.gov.ua/UJRN/VNULPX_2014_787_86

12. Sapir L., Stanley C. B., Harries D. Properties of Polyvinylpyrrolidone in a Deep Eutectic Solvent // The Journal of Physical Chemistry A. 2016. Vol. 120, Issue 19. P. 3253–3259. doi: 10.1021/acs.jpca.5b11927

13. Klimov V. V. Nanoplazmonika. Moscow: Fizmatlit, 2010. 480 p.

14. Boren K., Hafmen D. Pogloshchenie i rasseyanie sveta malymi chasticami. Moscow: Mir, 1986. 664 p.

15. The Optical Properties of Metal Nanoparticles: The Influence of Size, Shape, and Dielectric Environment / Kelly K. L., Coronado E., Zhao L. L., Schatz G. C. // The Journal of Physical Chemistry B. 2003. Vol. 107, Issue 3. P. 668–677. doi: 10.1021/jp026731y

16. Kreibig U., Vollmer M. Optical properties of metal clusters. Berlin: Springer-Verlag, 1995. 535 p. doi: 10.1007/978-3-662-09109-8

17. Polyvinylpyrrolidone (PVP) in nanoparticle synthesis / Koczkur K. M., Mourdikoudis S., Polavarapu L., Skrabalak S. E. // Dalton Transactions. 2015. Vol. 44, Issue 41. P. 17883–17905. doi: 10.1039/c5dt02964c

18. Yang C.-C., Wan C.-C., Wang Y.-Y. The Role of Poly(N-vinyl-2-pyrrollidone) in Ag⁄Pd Nanoparticles Formation and Its Application to Electroless Deposition // Journal of The Electrochemical Society. 2006. Vol. 153, Issue 5. P. J27. doi: 10.1149/1.2176917

Network characteristic of styrene-acrylic polymer films with Fe_3O_4 nanoparticles

Table 4

Network characteristic of nanopolymer film

Polymer film	Sol fraction S, %	Cross-linking degree *j*,%	Fraction of active chains *Vc*	Swelling degree *a*, %	Fraction of moist-free polymer in the swollen gel *Vr*
Tubifast 4010®	43.08	2.01	2433.98	14.05	0.07
Tubifast 4010® Tubifix	21.59	3.81	499.13	4.36	0.22
Tubifast 4010® Tubifix Nano Fe_3O_4	8.34	8.91	7.60	5.13	0.74

Table 4 shows that films based on styrene-acrylic polymer Tubifast 4010® are distinguished by a high degree of intermolecular cross-linking. Taking into account that the individual Tubifast 4010® film is unstable to solvents, the introduction of crosslinking agents increases the degree of structuring of the polymer. The 4 % concentration of Tubifix as the crosslinking agent gives the lowest in 5 times fraction of the active chains, which results in a significant increase in the crosslinking density of the polymer film.

Adding nano Fe_3O_4 as a filler to the polymer composition increased a degree of crosslinking approximately in 4 times. The fraction of active chains decreased approximately in 82 times.

Analyzing a swelling degree of the polymer films shows that swelling of film based on styrene-acrylic polymer Tubifast 4010® is on 31 % bigger than films with crosslinking agent according to the forming of crosslinking structure, and on 30 % bigger then film with nano Fe_3O_4 that can be explained by inorganic structure of Fe_3O_4 and an ability to form extra chains.

The styrene-acrylic polymer features presence of long flexible sections of molecules separated by carboxyl groups, which contribute to a strong local interaction between chains resulting in formation of linear structures (Fig. 2). Presence of carboxyl groups of methacrylic acid in the acrylic copolymer provides formation of an elastic polymer structure.

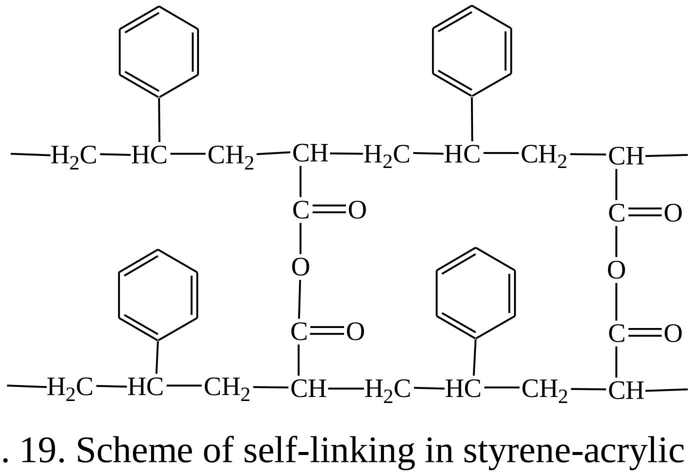

Fig. 19. Scheme of self-linking in styrene-acrylic polymer

When self-linking in styrene-acrylic polymers takes place (Fig. 19), not all carboxyl groups react. Therefore, admixtures of free acid monomers are deliberately added in industrial production of styrene-acrylic polymers to achieve maximum degree of interaction of the polymer with cross-linking agents.

In order to increase the degree of cross-linking in the styrene-acrylic polymer, a cross-linking agent (partially etherified melamine resin) was added (Fig. 20, film 2). In this case, interaction between the carboxyl groups of styrene-acrylic polymer and methylolene groups of the cross-linking agent is formed and a strong grid-type structure arises [10] (Fig. 20).

Introduction of cross-linking agents into the polymer composition indicates formation of a three-dimensional spatially "stitched" structure.

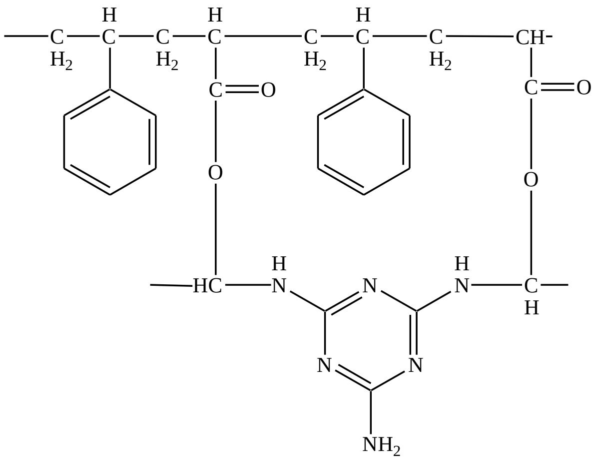

Fig. 20. Scheme of formation of a spatial structure of styrene-acrylic polymer and cross-linking agent

Free -NH_2 groups increase the resistance to non-polar solvents, to prevent this nano Fe_3O_4 was added to polymer composition as filler to create three-dimensional cross-linked structure. Forming a polar linking between -NH_2 groups and Fe_3O_4 nanoparticles can explains the high stability of such film in organic solvents.

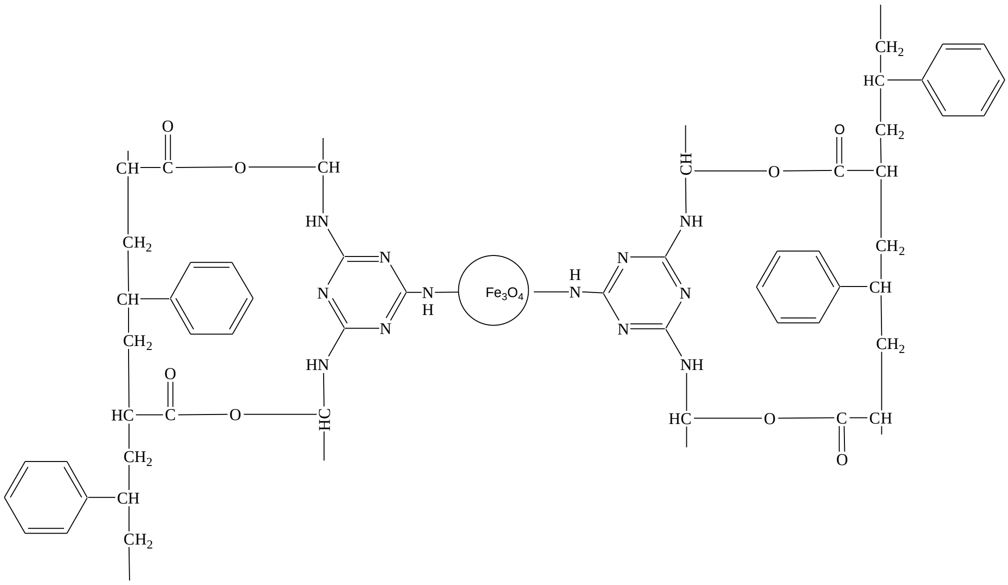

The basic idea in a composite is to integrate several component materials and their properties in a single material. In magnetic polymer nanocomposites, organic-inorganic synergies add new properties that cannot be achieved in just organic or inorganic materials. The magnetic component has nanometer dimensions, therefore its magnetic properties can differ qualitatively from the bulk, and they vary with the particle size. The polymer brings high processability, and interesting mechanical, optical, and electrical properties. In addition the magnetic properties can be strongly affected by the polymer interphase, and the capacity of polymers for structuring can be used to control the interparticle magnetic interactions. Thus, magnetic nanocomposites open a great number of possibilities for the design of materials in terms of reducing functional space, improving magnetic performance, modulating magnetic properties, multi-functionalization, and the development of materials with unique properties. The realization of these expectations passes through a better understanding of the physics at the nanometer scale, the development of characterization techniques, and the design of low cost production methods. This last is probably the most important challenge, because the performance of magnetic nanocomposites is very dependent on a fine control of size, size dispersion, shape, interface, and organization of the component materials.

Magnetic polymer nanocomposites may present a large variety of forms. Within each of these forms, they are designed to yield an optimal performance for a certain application. Following the basic chain in materials research in an inductive direction, the performance of composites is related to their properties, which are determined by their composition and structure, which are leading to the development of methods for their preparation. Thus, in the next section of this chapter, the different types of magnetic nanocomposites will be presented accordingly with this scheme. Then, in further sections, each of the elements of the materials research chain will be revised, starting with an exposition of methods for the synthesis of magnetic nanocomposites, and following with a description of the basic techniques for the characterization of their structure, and their main physical properties. Finally, we will comment on the future trends in this field.

Polymer nanocomposite films with Fe_3O_4 nanoparticles can be used as:

Magnetooptical materials

Magnetic nanoparticles showing Faraday rotation effect, and/or Kerr effect can be of interest in the fabrication of switches and devices. Size dependant transmittance and Faraday rotation have been found in maghemite ferrofluids and ferrite films. Multilayered assemblies of yttrium garnet nanoparticles show magnetization-induced second harmonic generation (Kerr effect). In metal/PMMA nanocomposites, the main absorption band narrows and additional peaks appear when decreasing the particle size.

Sensor applications

Nanocomposites of magnetic particles in isolating polymer matrixes show tunnelling magnetoresistance (TMR), and nanocomposites with a conductive polymer matrix exhibit giant magnetoresistance (GMR). Iron-poly(p-xylylene) nanocomposites display a significant magnetoresistance (36%) at room temperature. Nanocomposites of Fe_3O_4 in polyimide show magnetoresistance also in ac current (magnetoimpedance). Important advantages of polymer nanocomposites are the elimination of undesired eddy-current losses, and the protection from oxidation.

Ultrahigh density recording media

It is generally assumed that the next generation of magnetic recording materials will consist of a highly ordered arrangement of ferromagnetic nanoparticles, each of them supporting a bit. Polymer nanocomposites are good candidates, thanks to the extraordinary capability of polymers for templating and self-assembly. A magnetic nanocomposite film with a 5 nm grain size would provide a recording density as high as 1010 bit/cm2. Magnetite is a magnetic compound proposed for this application. The ordering can be achieved by self-assembly of nanoparticles coated with a surfactant, or by `in situ' growth of the particles in a block copolymer template. Materials consisting of nanocomposite grains embedded in a second polymer have also been proposed for magnetic recording. The performance of magnetic nanocomposites for magnetic recording can be improved by using elongated particles, with enhanced shape anisotropy, or ferro-antiferro core-shell particles (Co-CoO or Fe-FeO), that show a high magnetic stability thanks to exchange coupling between the two magnetic phases.

Membranes and sensors

Ordered films of magnetite in cellulose can be used as magnetic membranes, and assembled multilayers of clay, polymer polycations, and magnetite nanoparticles have been proposed as sensor arrays.

Synthesis and characterization of ZnO nanoparticles

ZnO nanoparticles were synthesized by direct precipitation method using zinc acetate ($Zn(CH_3COO)_2 \cdot H2O$) and sodium carbonate Na_2CO_3. In this work, the ethanol solution (0.1 M) of zinc acetate ($Zn(CH_3COO)_2 \cdot H2O$) and the solution (0.1 M) of Na_2CO_3 were prepared in ethanol, respectively. The Na_2CO_3 solution was slowly added into zinc acetate solution at room temperature under vigorous stirring, which resulted in the formation of a white suspension. The white product was centrifuged at 4000 rpm for 10 min and washed three times with distilled water. The obtained product was calcined at 300 °C for 30 min.

$$Na_2CO_3 + Zn(CH_3COO)_2 = 2Na(CH_3COO) + ZnCO_3$$

$$ZnCO_3 \rightarrow ZnO + CO_2$$

Then by using Photon cross-correlation spectroscopy average size of the particles was measured. Average size of nanoparticles is 45-55 nm.

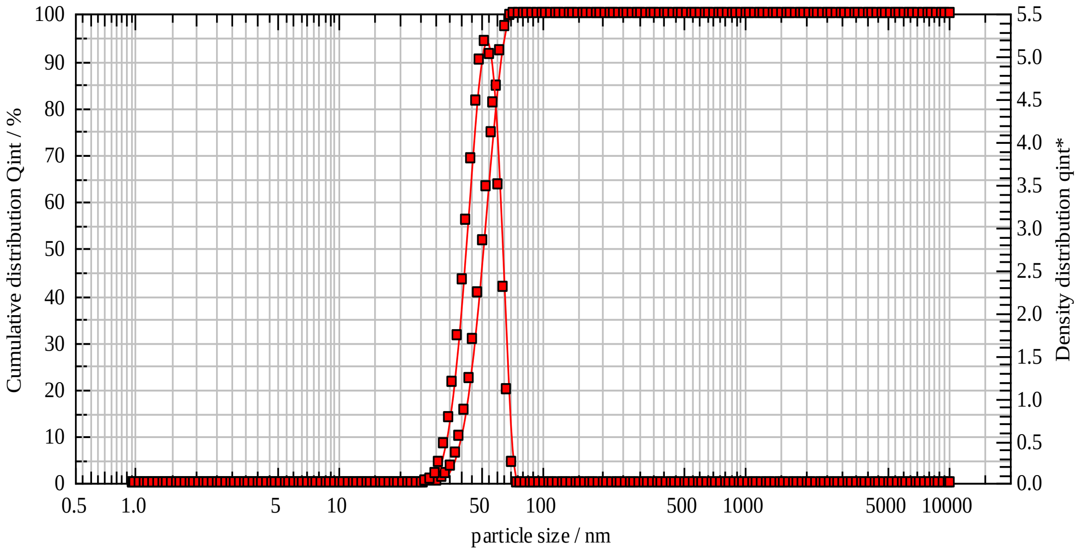

Fig. 21 Average size of the particles

The FTIR spectrum of ZnO was recorded in the range 350–4000 cm^{-1}, and it is given in Fig. 22. From the FTIR spectrum, various functional groups and metal-oxide bond present in the compound were analyzed. In the FTIR spectrum, a significant vibration band ranging from 400 cm^{-1} to 500 cm^{-1} is assigned to the characteristic stretching mode of ZnO bond. A broad peak at 3434 cm^{-1} (stretching) and 1330 cm^{-1} to 1670 cm^{-1} (bending) indicates the presence of hydroxyl residue which is due to atmospheric moisture [31,32].

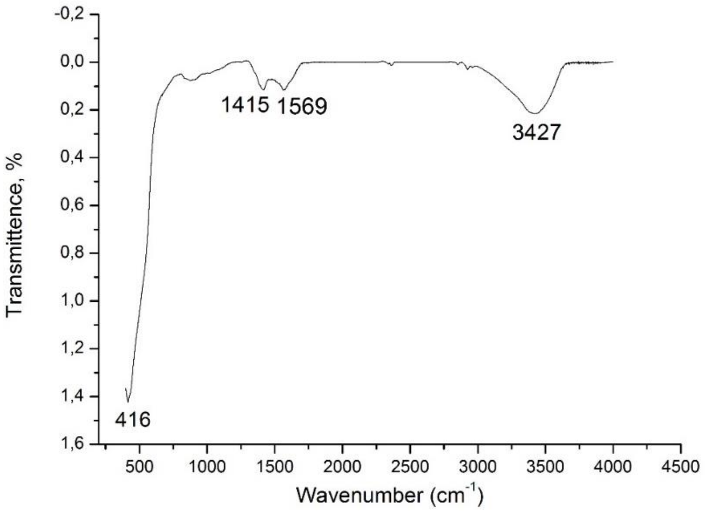

Fig. 22 FTIR ZnO nanoparticles

Network characteristics of polymer films with ZnO nanoparticles

Adding nano zinc oxide as a filler to the polymer composition a degree of crosslinking increased approximately in 4 times. The fraction of active chains decreased approximately in 82 times.

Table 5

Network structure of polymer film

Polymer film	Sol fraction S, %	Cross-linking degree *j*,%	Fraction of active chains *Vc*	Swelling degree *a*, %	Fraction of moist-free polymer in the swollen gel *Vr*
Tubifast 4010®	43.08	2.01	2433.98	14.05	0.07
Tubifast 4010® Tubifix	21.59	3.81	499.13	4.36	0.22
Tubifast 4010® Tubifix Nano ZnO	4.34	15.54	6.60	4.13	0.24

Analyzing a swelling degree of the polymer films shows that swelling of film based on styrene-acrylic polymer Tubifast 4010® is on 31 % bigger than films with crosslinking agent according to the forming of crosslinking structure, and on 30 % bigger then film with nano ZnO that can be explained by inorganic structure of ZnO and an ability to form extra chains.

Free -NH_2 groups increase the resistance to non-polar solvents, to prevent this nano ZnO was added to polymer composition as filler to create three-dimensional cross-linked structure. Forming a polar linking between -NH_2 groups and ZnO nanoparticles can explains the high stability of such film in organic solvents, and predict a good possibility to use such films for water treatment purpose.

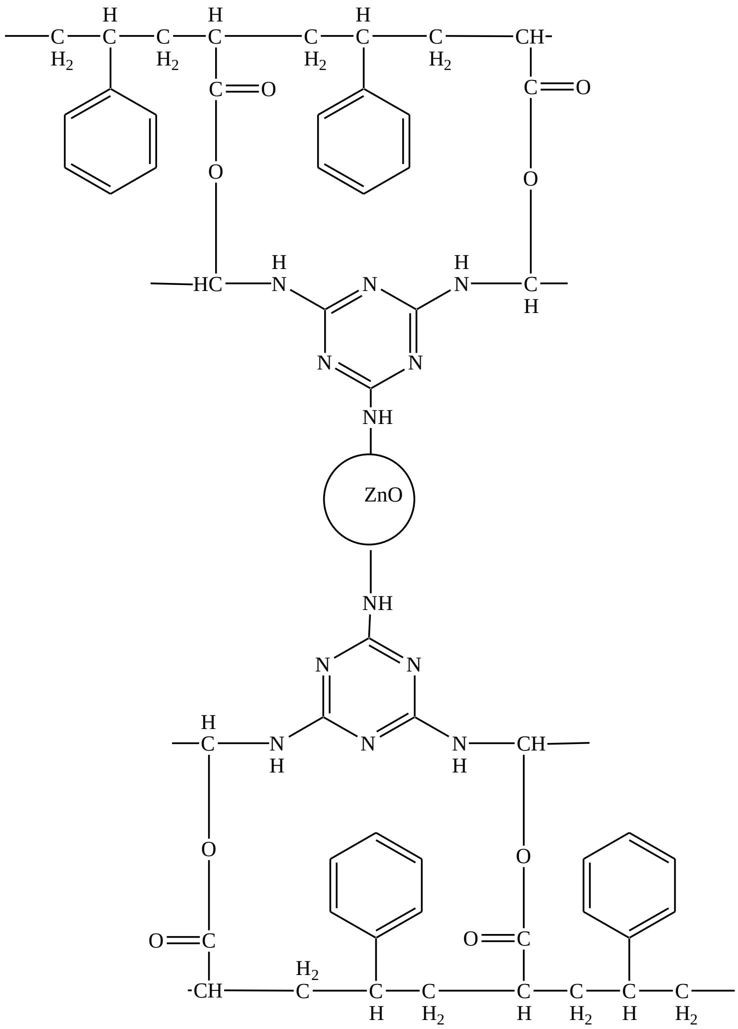

Fig. 23. Scheme of formation of a spatial structure of styrene-acrylic polymer, cross-linking agent and ZnO nanoparticles

Network structure of polymer film is confirmed by infrared spectroscopy obtained during the study (Fig. 23). The absorption bands at 3500-3300 cm^{-1} are referred to stretching vibration of NH_2 groups of PEMR; 3027 cm^{-1} to C-H vibrations of the phenyl ring of styrene; 2958, 2932 and 2873 cm^{-1} to asymmetric and symmetric C-H vibrations of alkyl groups, respectively; the intensive sharp band at 1729 cm^{-1} belongs to the C=O vibrations of SAC; the low-intensity band at 1602 cm^{-1} refers to stretching vibrations of the C=C in the aromatic rings of styrene. The absorption bands at 1453, 1377, 1030 cm^{-1} could be attributed to -C=N of PEMR; a band at 1158 cm^{-1} corresponds to stretching vibrations of C–O–C. From the spectrum, it is clear that cross-linking between components happens due to the etherification of carboxyl groups. Additional information about interactions we can obtain comparing the bending vibrations for NH_2 group at 1640-1670 cm^{-1} (Fig. 24). So, we can see an absorption band of deformation vibrations of aminogroups is shifted from 1642 to 1666 cm^{-1}, that could mean that NH_2 groups of PEMR interacted with styrol-acrylate polymer and/or ZnO nanoparticles. Vibration of ZnO nanoparticles are seen only in visible diapason 450 nm, that was confirmed by UV-Vis spectroscopy measurement (SF 56).

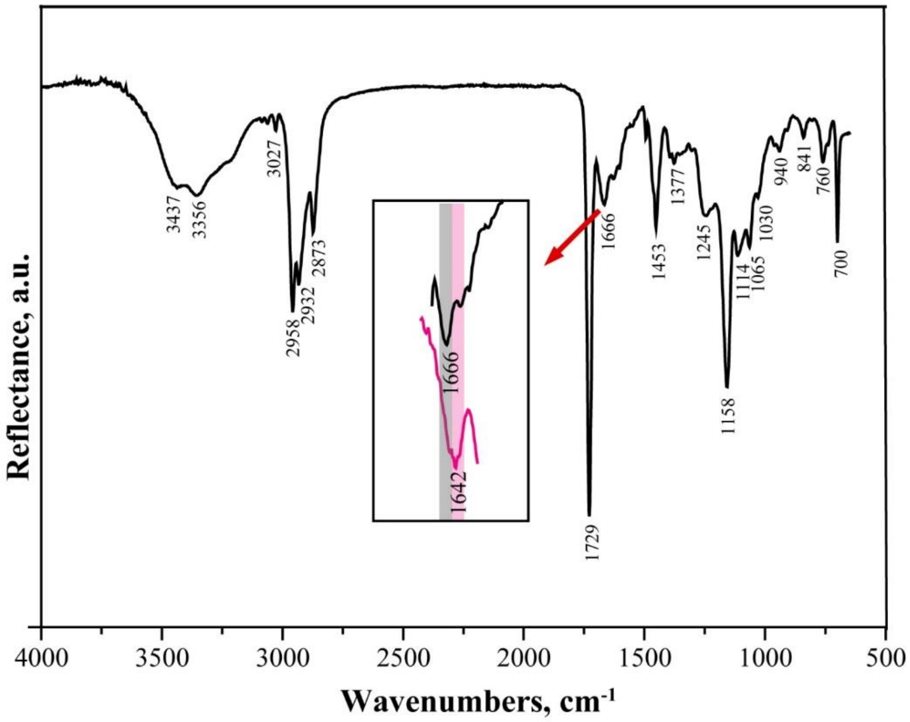

Fig. 24. FTIR spectrum of the composite material

Synthesized nanoparticles were investigated by X-ray diffraction. The patterns of ZnO nano particles shows that the diffraction peaks located at 31.8°, 34.44°, 36.32°, 47.6°, 56.71°, 62.96°, 68.13° and 69.18° have been keenly indexed as hexagonal wurtzite phase of ZnO (JPCDS card no: 36-1451), it also confirms the synthesized nano powder was free of impurities as it does not contain any characteristic XRD peaks other than ZnO peaks. The strong and narrow diffraction peaks indicate that the material has a good crystallinity and size

To calculate the average ZnO nanoparticles diameter Debye-Scherrer formula was used:

$$D = \frac{0,94 \bullet \lambda}{B \cos \theta}$$

The average particle size of the samples was about 16.21 nm. the plane (101) is found to be more intense than other peaks indicates the direction of crystal growth along the c axis (direction [0001]) of the ZnO wurtzite structure.

When ZnO nanoparticles involved in polymer composition the diffraction peak is decreased and shifts of approximately 1° in the peak positions. The broadening of difraction peaks in the XRD pattern is an indication for the presence of microstrain in the respective sample. This possible change in the peak intensities is due to a change in the electronic density in the crystallographic position. In this case, as is shown in Fig.2, shift in the XRD peak positions of ZnO is toward the higher 2θ values, indicating the presence of tensile strain in the sample.

Otherwise adding ZnO nanoparticles in polymer matrix involve aggregation of nanoparticles, they contribute and all the ZnO characterization peaks has the same longs and the average particle size is 25-45 nm.

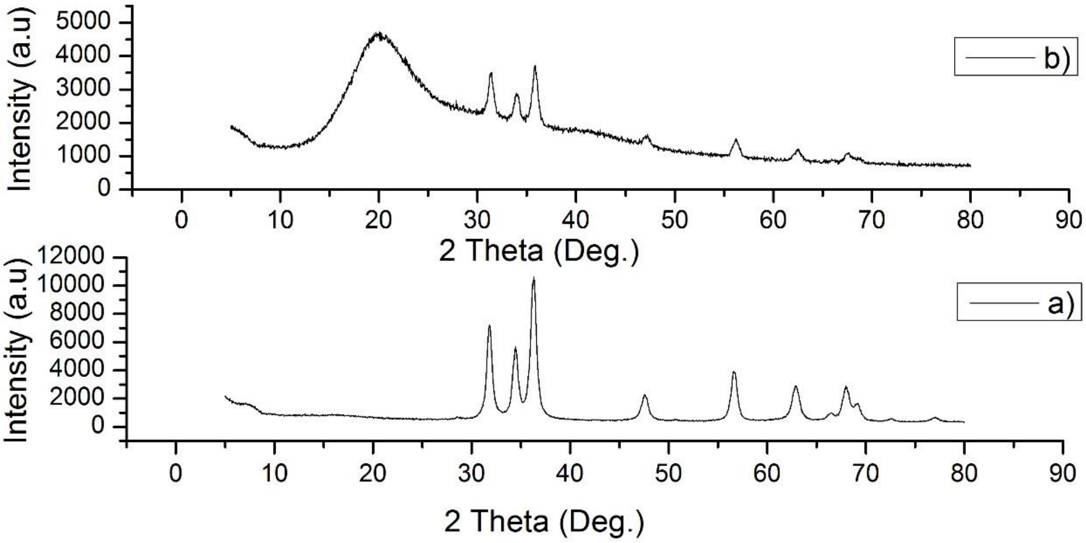

Fig. 25 XRD characterization of nanoparticles and polymer films

a) ZnO nanoparticles; b) polymer nanocomposite with ZnO nanoparticles

Swelling studies of polymer films with ZnO nanopartices

Dynamic and equilibrium swelling ratios were studied in 50 ml of distilled water (pH 7.5) at 40 ^{0}C. Dynamic study was performed up to 10 hours until the samples reached the constant mass. The swelling ratio of each filmwas calculated from the following relation

Swelling data provides additional insights into the relationship between network and crosslinking density. This supports the theory that a higher initial double bond concentration produces a more densely crosslinked network.

Swelling studies were performed to investigate the degree of crosslinking and the degradation kinetics of theacrylates networks. The film samples were dissolved in water and the dissolution was monitored over time at room temperature using a simple gravimetric method. Four identical samples were prepared. The remaining crosslinked films were placed in 20 mL distillate water and were used for degradation and swelling studies. At selected time intervals, films were removed from solution and were patted dry and weighed to determine swollen mass (Ms). The films were then dried in oven and weighed to determine final dry mass (Mfd). The swelling degree of each film was calculated using the equation:

$$Sd = \frac{Ms - Mfd}{Mfd} \bullet 100,$$

Where Ms is the weight of the swollen film and Mfd is the weight of the final dried film.

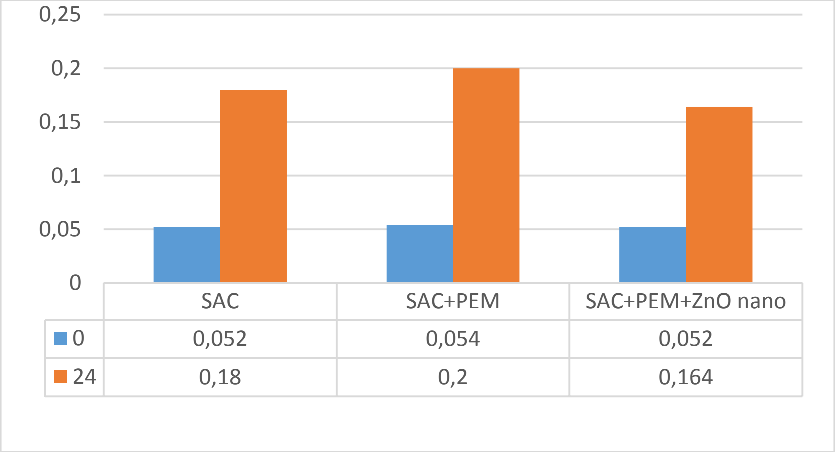

	SAC	SAC+PEM	SAC+PEM+ZnO nano
🟦 0	0,052	0,054	0,052
🟧 24	0,18	0,2	0,164

Fig. 26 Swelling of polymer films

As it described on the graph (Fig. 26), films with a higher mass percentage of acrylates dissolved more slowly than those with a smaller amount of acrylate. This effect is explained by consideration of the crosslinking density in the formed films.

In Lakrytex 273 the initial double bond concentration is higher therefore, the denser crosslinking sites, help to form tighter interpenetrating networks, resulting in slower dissolution rate due to the difficulty for water to penetrate the network. Lakrytex 333did not form stable crosslinked film under identical conditions, it have a high value of swelling degree so this justify that polymer didn’t form crosslinking network and dissolve in solvents. As Lakrytex 273 and 430 have a high crosslinking degree and didn’t dissolve in solvents they have lower value of swelling degree.

A self-crosslinked film is formed, by a regular covalent bonds. The behavior depend on the tightness of the network; network such as shown in Figure 26 would exhibit less swelling than the network without crosslinked unites. Even with such models for an "ideal" homogeneous unimolecular network, however, a problem arises, for in many real cases the lengths of chains between crosslinks may vary depending on the structure of the monomers or prepolymers, or on the vagaries of reaction kinetics. Of particular interest to the next studyof crosslinking is the influence of the effect of a distribution in the mass of the polymer film. Furthermore, a real polymer network is usually quite different from the ideal in structure. Not only do loops and dangling chain ends detract from the effectiveness of the structure, but shorter chains, either linear or branched, may exist without direct chemical connection to the network.

Created multifunctional materials with inorganic nanoparticles can be used as building materials, corrosion-resistant, heat-resistant and fire resistant coatings, packaging materials with low gas permeability and different household products.

Technology of production of multifunctional materials can find many uses, especially in areas where the unique properties of the material are more important than its cost. However, it should not be forgotten that new technologies are more difficult than old, so their development will require a qualitative leap in training a new generation of engineers and technologists.

Scanning Electron Microscope (SEM)

A scanning electron microscope scans electron beam across the sample surface and collects scattered electrons for imaging. Because the image is formed using backscattered signals instead of forward-transmitted signals, the electron beam energy does not need to be high (<40 keV) and the sample also does not require electronic transparency; it has only a conductivity requirement to prevent charging. At least four different kinds of signals are scattered backwards that we can potentially use: secondary electrons, backscattered electrons, and characteristic X-ray and Auger electrons. The most popular SEM imaging method is secondary electron imaging or SEI. SEI can produce good resolution imaging down to 1 to 5 nm with a large depth of field—this feature helps reveal much information about surface topography. On the other hand, backscattered electrons are often scattered by samples elastically and thus is strongly related to atomic number (Z) near the surface as well as crystallographic orientation of the surface. Therefore, backscattered electrons are often used to identify chemical composition together with characteristic X-rays. In fact, backscattered electrons are also used to image the distribution of elements with significant difference in weight for the same reason. For example, it is almost impossible for SEI to image colloidal gold with a radius of 1 to 5 nm decorated in biospecimen, whereas backscattered electron imaging can easily distinguish these elements due to different atomic numbers. Today, backscattered electrons are also used to detect surface orientation to construct a texture map for the specimen under study. Characteristic X-rays have also been widely used in SEM to identify materials chemical composition. This is called energy-dispersive X-ray spectroscopy or EDX. As discussed previously, the wavelength of the characteristic X-ray is directly related to the energy delta between the outer and inner shells of atoms and thus is a characteristic feature of elements.

Surface morphology of polymer nanocomposite films were measured by field emission scannig electron microscopy MIRA 3 FE-SEM microscope (TESCAN, Czech Republic) equipped with a high-resolution cathode (Schottky field emitter) and with three-lens Wide Field Optics^{TM} design.

SEM has been applied for the surface examination and characterization of polymer-ZnO films. The samples were mounted on a stub of metal with adhesive carbon tape and then observed in the microscope. During the experiments, SEM images of nanocomposites have been taken in different magnification. The SEM images indicate that homogeneous/heterogeneous dispersion of ZnO nanaparticles in polymer film.

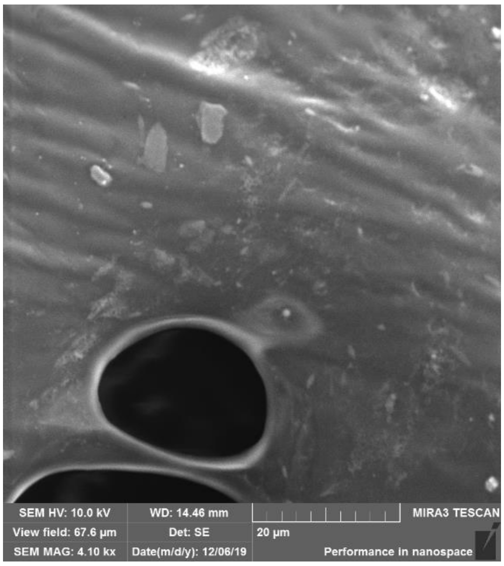

Fig 27 SEM images of polymer films with ZnO nanoparticles

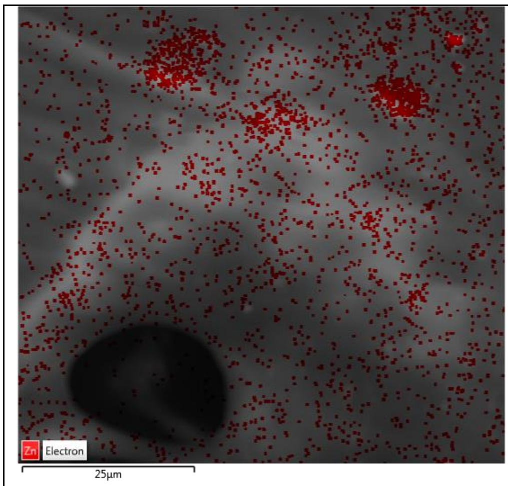	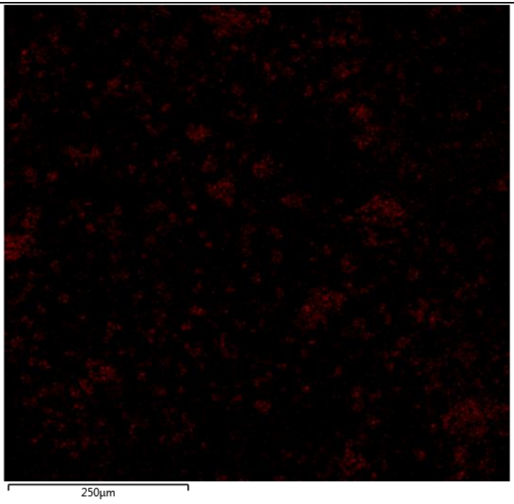
Fig. 28 Mapping of polymer films with ZnO scale 25	Fig. 29 Mapping of polymer films with ZnO scale 250

Conclusion

It was determined that films based on styrene-acrylic polymer cross-linking agent and nano Fe_3O_4 have a high degree of intermolecular cross-linking 8.92 %. Individual polymer films formed from styrene-acrylic polymer Tubifast 4010® are not able to provide quality characteristics to a polymer film, and therefore require the addition of cross-linking agents. An interaction between an active chains of the components of polymer composition was shown. To prevent the resistance of free -NH_2 groups of cross-linking agent to non-polar solvents nano Fe_3O_4 was added to polymer composition as filler to create three-dimensional cross-linked structure. Forming stable grid-type structure in polymer film predetermines good opportunities to use such films in fields where magnetic properties are necessary.

It was determined that films based on styrene-acrylic polymer cross-linking agent and nano ZnO have a high degree of intermolecular cross-linking 15.54%. To prevent the resistance of free -NH_2 groups of cross-linking agent to non-polar solvents nano ZnO was added to polymer composition as filler to create three-dimensional cross-linked structure. Forming stable grid-type structure in polymer film predetermines good opportunities to use such films in water treatment technologies were the cross-linked ZnO nanoparticles can exhibit photocatalytic activity.